DRD LINE ITEM NO. SE-7

DOE /JPL-954929-84/11

PHOTOVOLTAIC CELL RELIABILITY RESEARCH

FIFTH ANNUAL REPORT
SEPTEMBER 1984

J.W. Lathrop
Department of Electrical and Computer Engineering
Clemson University
Clemson, SC 29631

PREPARED FOR
JET PROPULSION LABORATORY

PREPARED BY
CLEMSON UNIVERSITY

DRD Line Item No. SE-7

DOE/JPL - 954929-84/11

ENGINEERING AREA

PHOTOVOLTAIC CELL RELIABILITY RESEARCH

INVESTIGATION OF ACCELERATED STRESS FACTORS AND FAILURE/DEGRADATION MECHANISMS IN TERRESTRIAL SOLAR CELLS

FIFTH ANNUAL REPORT

J.W. Lathrop

Department of Electrical and Computer Engineering
Clemson University, Clemson, SC 29631

September 1984

The JPL Flat-Plate Solar Array Project is sponsored by the U.S. Department of Energy and is part of the Photovoltaic Energy Systems Program to initiate a major effort toward the development of cost-competitive solar arrays. This work was performed for the Jet Propulsion Laboratory, California Institute of Technology by agreement between NASA and DOE.

CLEMSON PERSONNEL

Persons contributing to the work covered in this report include:

Dr. Jay W. Lathrop	Principal Investigator
Mr. Dexter C. Hawkins	Research Associate
Ms. Clara White Davis	Graduate Student (cell measurement techniques)
Mr. William G. Stoddard	Graduate Student (a-Si cell testing)
Mr. Thomas A. Bolin	Undergraduate Student
Mr. H. Jarrett Cassell, Jr.	Undergraduate Student
Mr. Michael A. Cross	Undergraduate Student
Mr. Thomas A. Hipp	Undergraduate Student
Mr. Scott F. LaFave	Undergraduate Student
Mr. Paul A. Williamson	Undergraduate Student

ACKNOWLEDGEMENT

The Jet Propulsion Laboratory Technical Manager for this work was Mr. Edward L. Royal. His assistance in acquiring test samples and in supplying technical guidance to the program is gratefully acknowledged.

Preliminary

ABSTRACT

This annual report presents results of an ongoing research program into the reliability of terrestrial solar cells. The main focus of the research is to identify failure/degradation modes affecting solar cells and to relate these to basic physical, chemical, and metallurgical phenomena. The program is concerned with the reliability attributes of individual single crystalline, polycrystalline, and amorphous thin film silicon cells. Results of subjecting different types of crystalline cells to the Clemson accelerated test schedule are given. Preliminary step stress results on one type of thin film amorphous silicon (a:Si) cell indicated that extraneous degradation modes were introduced above 140 C. The report also describes development of measurement procedures which are applicable to the reliability testing of a:Si solar cells. An approach to achieving the necessary repeatability, currently being explored, of fabricating a simulated a:Si reference cell from crystalline silicon photodiodes is described.

TABLE OF CONTENTS

Section	Page
CLEMSON PERSONNEL	ii
ACKNOWLEDGEMENT	iii
ABSTRACT	iv
TABLE OF CONTENTS	v
LIST OF FIGURES	vi
LIST OF TABLES	vii
1.0 INTRODUCTION	1
2.0 RELIABILITY RESEARCH TEST PROGRAM	5
2.1 Exploratory Reliability Testing of Unencapsulated a:Si Cells	5
2.2 Crystalline Cell Reliability Research	15
2.3 Outdoor Real-Time Testing of Individual Cells	30
3.0 a:Si RELIABILITY INSTRUMENTATION RESEARCH	33
3.1 General Considerations	33
3.2 Simulated a:Si Standard Cells	35
3.3 Large Area Light Source	37
3.4 System Configuration and Data Acquisition Procedures	46
3.5 Second and Fourth Quadrant Measurement	52
3.6 Low Temperature Measurement Jig for Crystalline Si Cells	54
3.7 New Clemson Reliability Research Facility	59
4.0 CONCLUSIONS	61
5.0 NEW TECHNOLOGY	63
6.0 PROGRAM RESEARCH CONTRIBUTIONS	65
7.0 REFERENCES	67
APPENDIX A. Publication Abstracts	69

List of Figures

Figure		Page
1.	Photograph of Measurement Jig for 16-Cell a:Si Submodule	7
2.	Step Stress Schedule for a:Si Cells	8
3.	Histogram of Average Power Degradation of 16-Cell a:Si Submodule Following Step Stress Schedule	11
4.	IV Characteristics of a:Si Cells Before and After Step Stress Testing	13
5.	Crystalline Cell Test Schedule Key to Summary Data Tables	16
6.	Photograph of Outdoor Real Time Test Rack	31
7.	Approach to a Simulated a:Si Standard Cell Using Filtered Crystalline Silicon Photodiodes	36
8.	Average Measured Intensity Variation of ELH Lamps	39
9.	Calculated Intensities Over an Extended Area for an 11-Lamp ELH Array	40
10.	Lamp Location Diagram for 11-Lamp Array	41
11.	Original Measured Intensity Variation of 11 Lamp Array	43
12.	Measured Intensity Variation of 11-Lamp Array after Lamp Tilt Adjustment	44
13.	Intensity Monitoring and Adjustment System Schematic	45
14.	Multivapor Lamp Spectral Characteristics	47
15.	Block Diagram of the a:Si Short Interval Tester	48
16.	Photograph of the a:Si Short Interval Tester	49
17.	Flow Diagram of Data Taking Routine for AC Lamp Simulator	50
18.	Timing Diagram of AC Light Source Data Acquisition Technique	51
19.	Comparison of AC and DC Data Collection Methods	53
20.	Power Supply Modification for 4th Quadrant Operation	55
21.	Graphical Representation of 2nd, 3rd, and 4th Quadrant Data	56
22.	Photograph of Low Temperature Measurement Jig for Crystalline Cells	58
23.	Photograph of Clemson's Auger Microprobe	60

LIST OF TABLES

Table		Page
1	Result of Step Stress Testing a:Si Cells	10
2	Unencapsulated Cell Types Classified by Primary Metallization	17
3A	Unencapsulated Cell Bias-Temperature Test Results (maximum power output, N-, O-, and P-cells)	18
3B	Unencapsulated Cell Bias-Temperature Test Results (maximum power output, Q-, R-, and V-cells)	19
3C	Unencapsulated Cell Bias-Temperature Test Results (maximum power output, W-, and X-cells)	20
3D	Unencapsulated Cell Bias-Temperature Test Results (maximum power output, Y- and Z-cells)	21
4	Unencapsulated Cell B-T Test Results (catastrophic mechanical change)	22
5	Unencapsulated Cell 85 C/85 %RH Test Results (maximum power output degradation)	23
6	Unencapsulated Cell 85 C/85 %RH Test Results (catastrophic mechanical change)	25
7	Unencapsulated Cell Pressure Cooker Test Results (maximum power output degradation)	26
8	Unencapsulated Cell Pressure Cooker Test Results (catastrophic mechanical change)	28
9	Summary of Unencapsulated Crystalline Cell Accelerated Test Results	29
10	Unencapsulated Cell Real-Time Test Results (maximum power degradation)	32

omit

1.0 INTRODUCTION

This is the Fifth Annual Report on the Investigation of Accelerated Stress Factors and Failure/Degradation Mechanisms in Terrestrial Solar Cells, a photovoltaic cell reliability research program which has been conducted by Clemson University for the Department of Energy (DOE) Flat-Plate Solar Array (FSA) Project managed by the Jet Propulsion Laboratory. The objective of the research is the identification and characterization of fundamental physical, chemical, and metallurgical phenomena which, acting at the cell level, could cause photovoltaic modules to degrade with time. The approach followed is to develop laboratory tests which will accelerate the anticipated field failure modes, and then to subject quantities of different types of cells to these tests. Analysis of the pre- and post-stress test data, combined with visual observations, is then used in an effort to determine the nature of degradation mechanisms. The program was initiated in December of 1977 and earlier reports (1,2,3,4,5) have discussed the experimental and analytical methods employed, the data collected, and a number of preliminary conclusions. Prior to this reporting period, work had been concentrated entirely on crystalline silicon cells, with testing being performed on both encapsulated and unencapsulated configurations.

Technical activity of the reliability research program can be divided into the stress testing of cells (Section 2.0) and the development of instrumentation (Section 3.0). Amorphous silicon (a:Si) cell types have recently been included in the cell test program. Very little is known concerning the long term life of these cells and its effect on the reliability

of thin film modules, a problem now being investigated by JPL. Consequently the Clemson program has begun a study of their reliability attributes and some preliminary results are given in Section 2.1. The crystalline cell test program is continuing as well and Section 2.2 gives complete test results on 10 unencapsulated cell types that had only been partially reported on in the 4th Annual Report. Preliminary results on two new silicon ribbon cell types are also included in this section. These cell types are of particular interest to the program because of their potential for low cost and high efficiency. Real time outdoor testing is also underway. A test rack has been fabricated and numbers of individual cells, both encapsulated and unencapsulated installed. Results of this ongoing work are discussed.

Instrumentation development during the report period concentrated on a:Si measurement methods. Because of differences in their electrical and physical characteristics, the measurement techniques used to obtain a-Si reliability data must be quite different from those used with crystalline cells. Of prime concern is the absence of a stable a:Si reference cell for assuring illumination repeatability. Section 3.2 discusses an approach to reference cell fabrication using filtered single crystal silicon photo diodes. Because a:Si cells have a different form factor from crystalline cells it is necessary that the laboratory simulator be capable of uniformly illuminating a larger area. Ideally this illumination should also correspond to the spectral sensitivity of a:Si cells. However, cost and stability considerations favor an extension of the modular ELH approach used successfully for many years in crystalline reliability measurements. Development of a prototype large area simulator for use with a:Si cells is described in Section 3.3. The final system configuration of the a:Si measurement system and how it will be used

for data acquisition is described in Section 3.4.

Crystalline cell measurement techniques were upgraded during the reporting period in two important ways: 1) data taking and display of the associated IV curves was extended to include portions of the second and fourth quadrants, and 2) a jig was designed and fabricated which allowed characteristic curves to be measured at low temperatures. These developments are discussed in Sections 3.5 and 3.6 respectively. Finally, the new electron microscope facility at Clemson has become operational as discussed in Section 3.7. It is expected that the analytical capability of this instrumentation will prove to be extremely valuable in the analysis of degraded devices, permitting the fundamental mechanisms to be identified.

2.0 RELIABILITY RESEARCH TEST PROGRAM

2.1 Exploratory Reliability Testing of Unencapsulated a:Si Cells

In addition to requiring repeatable measurement techniques an accelerated test program must also select stress levels which will accelerate failure mechanisms expected in the field. If the stress level is too low the acceleration factor will be too small and an inordinate length of time will be required before changes are observed. On the other hand, if the stress level is too high, extraneous degradation mechanisms will be introduced which would never occur in the field in real time. Thus for an accelerated test program to be effective a stress "window" must exist. One method of determining if a window exists when there is no previous history, as is the case with a:Si cells, is to run a step stress test. In a step stress test the component is first measured, then subjected to a particular level of stress for a relatively short time. The component is then measured to determine if any changes have occurred and then subjected to a somewhat greater stress for a similar length of time. This second level of stress should be sufficiently high that its effect would be greatly in excess of any effects from the first stress level. Temperature stress effects are governed by the well known Arrenhius equation, which can be used to calculate the stress levels so there will be little cumulative effect, provided the activation energy can be estimated. Thus stress is increased in a step-wise fashion many times until significant change is observed signaling the onset of an extraneous degradation mode. In this way the test is able to give an indication of an upper stress level for accelerating real time phenomena.

Step stress investigations were conducted in order to obtain information concerning the permissible upper temperature stress levels for amorphous cells. Electrical measurements were made with the 4-lamp ELH simulator and short interval tester used for crystalline cell testing. A crystalline standard cell was used to initialize the simulator intensity prior to each measurement. While this method can result in absolute measurement error at any given step, as will be discussed in Section 3, the changes being sought were sufficiently great that it should still allow a good assessment of the temperature at which an extraneous degradation mode occurs.

Amorphous cell samples consisting of 16 relatively small (4.5 X 1 cm) a:Si cells fabricated on a common superstrate were obtained from a commercial manufacturer for use in the step stress investigation. This type of cell has been designated aA, where the lower case "a" prefix indicates amorphous silicon construction. The cells were not interconnected and could be individually contacted from the back. Figure 1 is a photograph of the jig used to contact the cells during measurement. A Kelvin probe arrangement of beryllium copper contacts was used. This type of localized metallic contact tended to scratch the thin film metallization. In addition, because the contacts were localized the current was not well distributed across the thin metallized areas. Future contacts will utilize conductive elastic material which will make possible extended contacts rather than point contacts.

The sixteen a:Si cells were photographed and electrically measured. The cells were then placed in an ambient air oven at 90 C for 20 hours and then again measured and photographed. This sequence was repeated at 10 C intervals through 150 C as illustrated in Figure 2. Results of the electrical

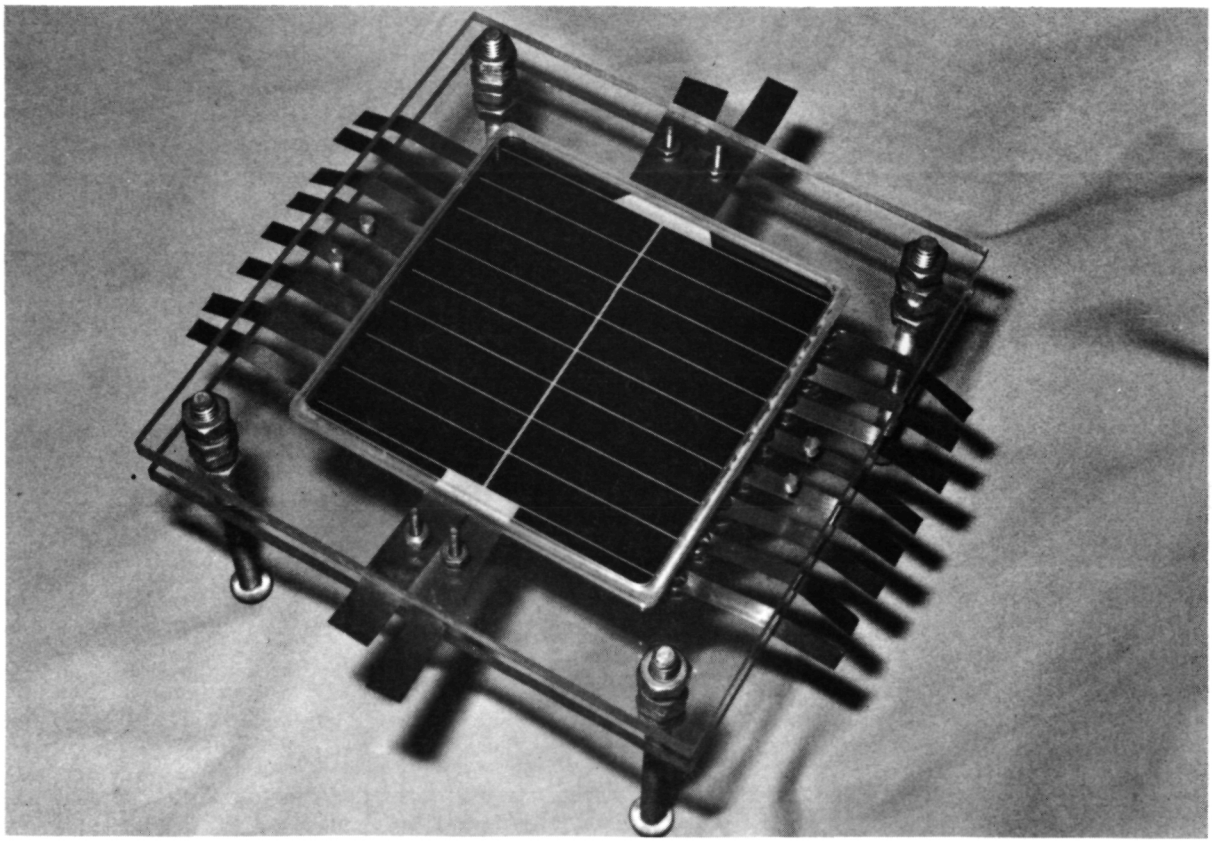

Figure 1. Photograph of Measurement Jig for 16-Cell a:Si Submodule

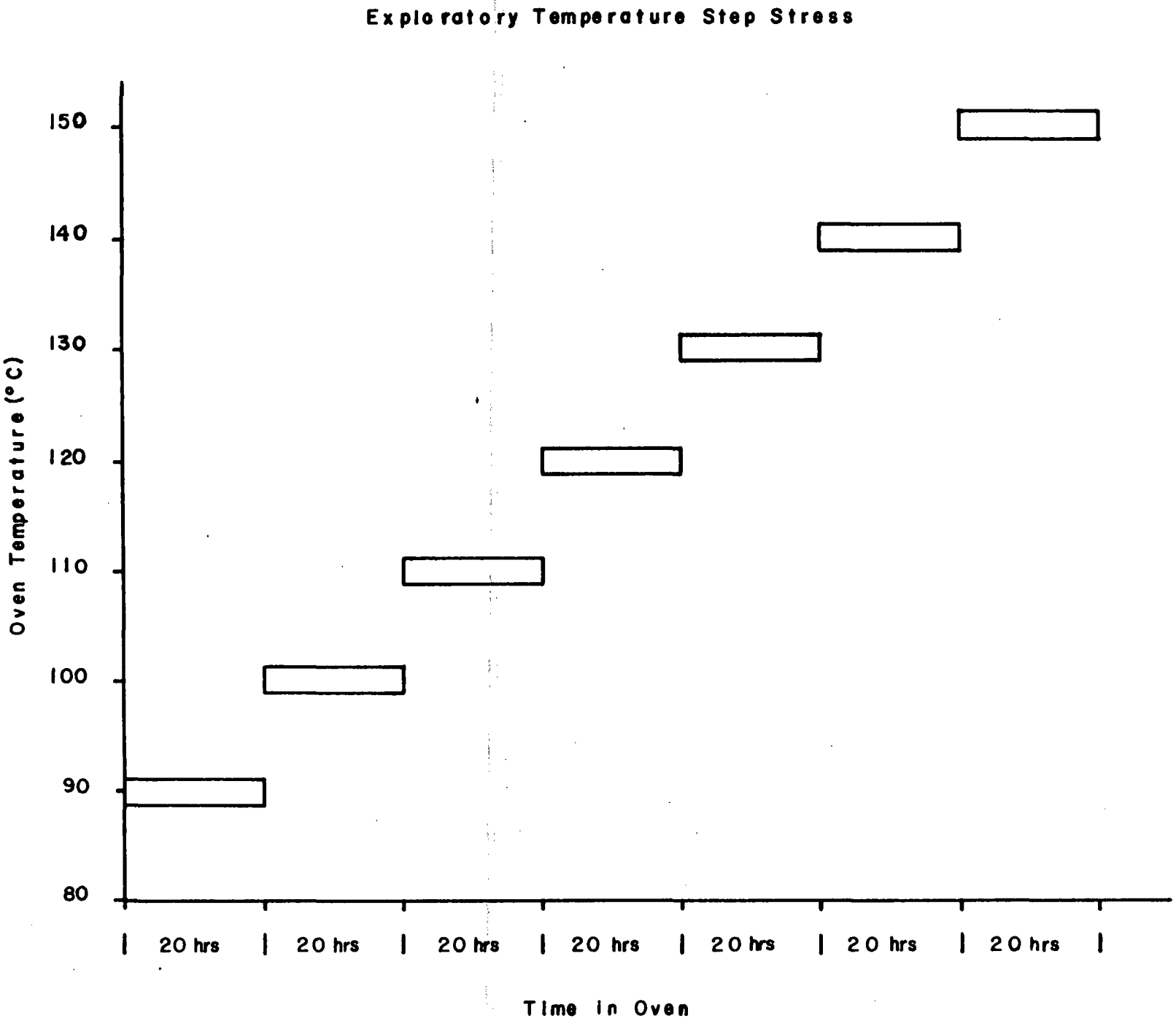

Figure 2. Step Stress Schedule for a:Si Cells

measurements are given in Table 1 and the histogram of Figure 3. It can be seen that while only small changes were observed through the 130 C step, a drastic decrease in Pm occurred as a result of the 140 C step. Individual IV curves of the 16 cells after the 140 C step are shown in Figure 4. An examination of color photographs taken before and after each step indicated that a subtle color change had occurred after the 140 C step. The change was too subtle to be reproduced in this report, but it was clear that the normally rosy color of the cell had a decidedly greenish tinge after the 140 C step.

It is apparent from the characteristic curves of Figure 4 that a reduction in Voc was the major reason for the observed power degradation. The reason for this reduction is not known, but it has been determined that it is accompanied by an increase in cell leakage of several orders of magnitude. Additional samples and other cell constructions will need to be tested before it can be determined whether this type of behavior is unique to these 16 cells or to this cell type. Based on these tests, however, there would be reason to question the validity of accelerated testing this type of cell above 130 C. Such a restricted "window" would limit the usefulness of accelerated testing, as discussed above, for evaluating the reliability attributes of a:Si cells. Crystalline cells have an upper temperature limit, limited by the melting point of solder, which is in excess of 155 C.

TABLE 1
RESULT OF STEP STRESS TESTING a:Si CELLS

Stress	% decrease (average of 16 cells) Voc	Isc	Pm
20 hours @ 90 C	-0.2	0.0	-1.4
20 hours @ 100 C	-0.7	0.3	-0.7
20 hours @ 110 C	-0.6	0.4	0.6
20 hours @ 120 C	0.7	0.5	1.1
20 hours @ 130 C	-0.7	0.8	0.4
20 hours @ 140 C	54.5	9.7	70.9
20 hours @ 150 C	86.3	29.6	94.2

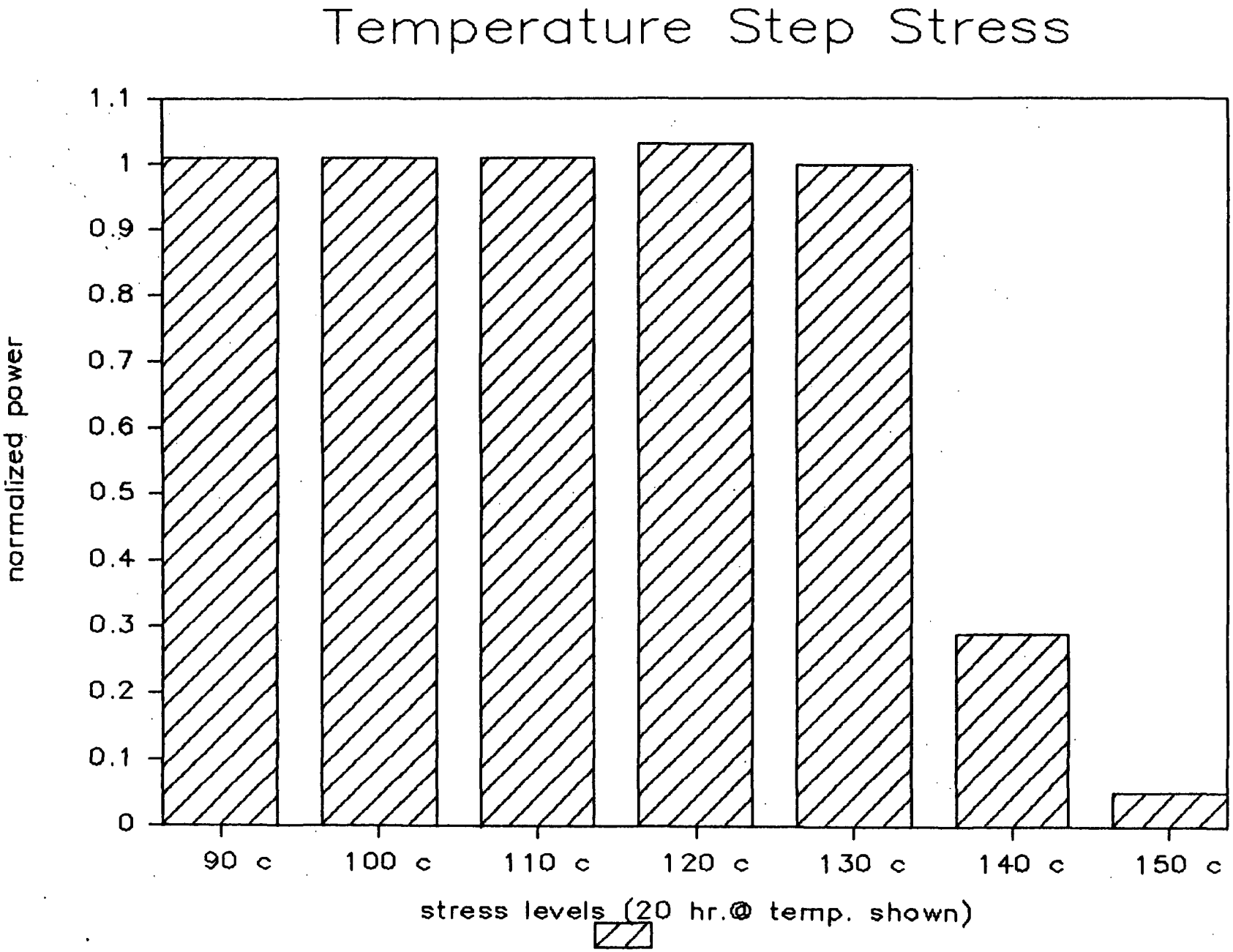

Figure 3. Histogram of Average Power Degradation of 16-Cell a:Si Submodule Following Step Stress Schedule

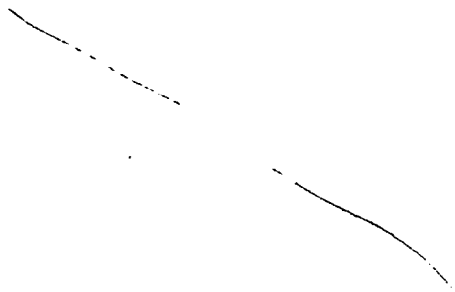

Page intentionally left blank

Page intentionally left blank

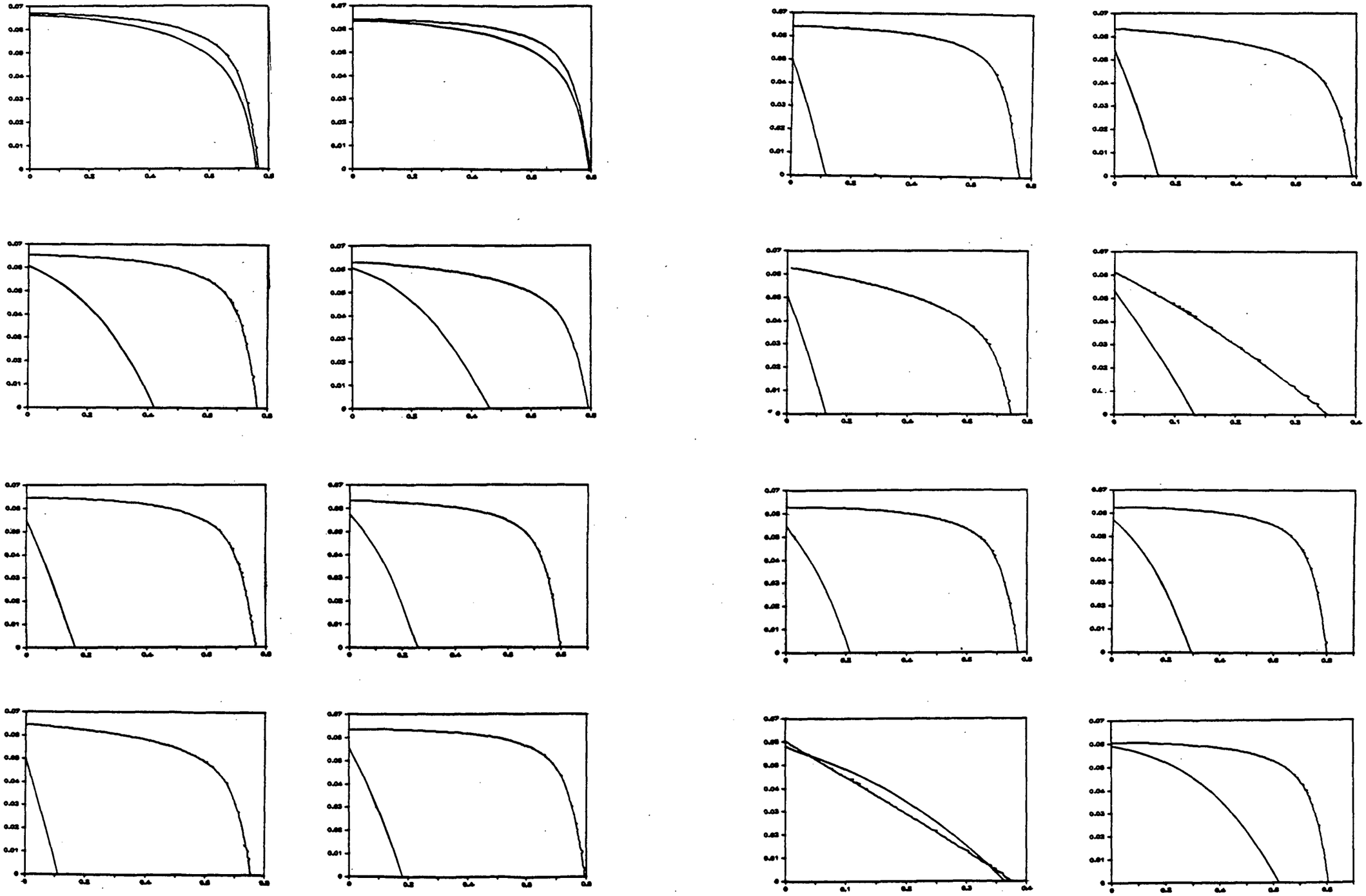

Figure 4. IV Characteristics of a:Si Cells Before and After Step Stress Testing

"PAGE MISSING FROM AVAILABLE VERSION"

2.2 Crystalline Cell Reliability Research

Partial results were reported in the 4th Annual Report on 10 unencapsulated crystalline cell types which were undergoing accelerated testing. Testing of these cells has now been completed and the final test results are given in the summary data tables which follow. Table 2 classifies the cell types according to the type of metallization each used and Figure 5 provides an overview of the summary data tables as an aid to the reader. A brief, rather subjective, summary of results on these 10 cells is given in Table 9.

Two new unencapsulated cell types were received during the reporting period and were started into test. Both cell types are of ribbon construction -- one being EFG and the other dendritic ribbon. At this time insufficient hours have been accumulated to establish any clear trends.

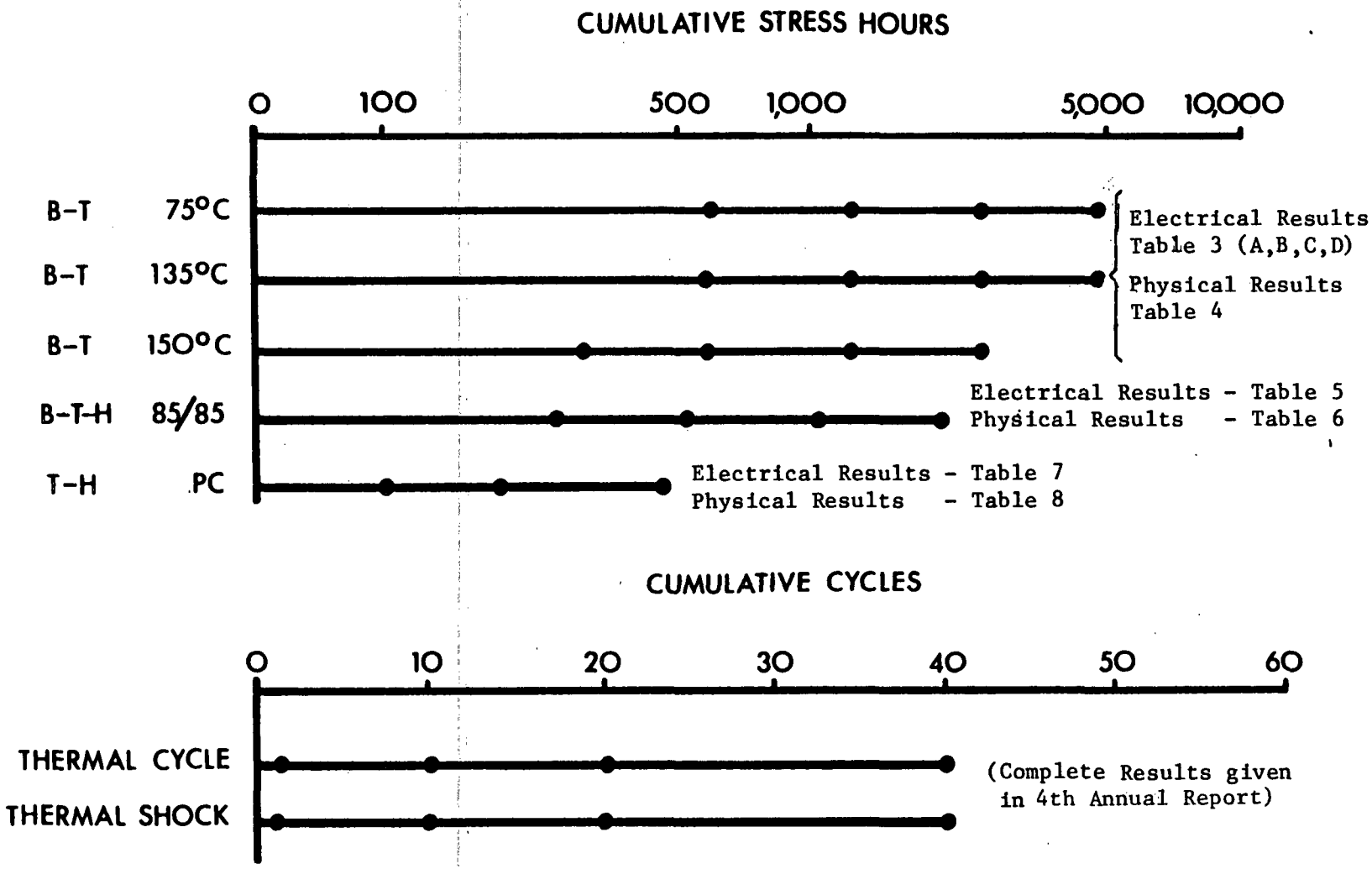

Figure 5. Crystalline Cell Test Schedule Key to Summary Data Tables

TABLE 2.

UNENCAPSULATED CELL TYPES
CLASSIFIED BY PRIMARY METALLIZATION

CELL TYPE	CONDUCTING LAYER	SOLDER
N	nickel plate	yes
O	nickel plate	yes
P	nickel plate	yes
Q	nickel plate	yes
R	copper plate	no
V	copper plate	yes
W	nickel plate	yes
X	nickel plate	yes
Y	silver paste	no
Z	silver paste	no

TABLE 3A
UNENCAPSULATED CELL BIAS TEMPERATURE TEST RESULTS
MAXIMUM POWER OUTPUT N-, O-, AND P-CELLS
(Test completed)

Cell	Temp C	Time (hr)	Total Cells	Range of Maximum Power Degradation 0-2%	3-9%	10-19%	20-29%	30-49%	50-100%
N	75	600	25	23	2				
		1200	25	3	8	4	10		
		2400	25	4	7	4	9	1	
		4800	23	2	9	3	9		
N	135	600	20	19	1				
		1200	20	19	1				
		2400	19	14	5				
		4800	18	9	8	1			
N	150	300	19	15	4				
		600	18	11	7				
		1200	15	5	8	2			
		2400	14	3	6	4	2		
O	75	600	25	19	6				
		1200	24		9	10	3	2	
		2400	24		9	10	2	3	
		4800	23		5	10	6	2	
O	135	600	20		14	6			
		1200	20		9	10	1		
		2400	20		6	12	2		
		4800	19		1	16	2		
O	150	300	20		14	6			
		600	20		9	11			
		1200	19		3	10	5	1	
		2400	17			1	1	12	3
P	75	600	25	17	8				
		1200	24	15	8	1			
		2400	24	19	5				
		4800	24	-1	-3				
				8	9	2	1		
P	135	600	20	15	5				
		1200	20	18	2				
		2400	20	17	3				
		4800	15	-1	-1				
				7	5	1			
P	150	300	20	20					
		600	20	20					
		1200	20		data erratic				
		2400	19	7	10	2			

TABLE 3B
UNENCAPSULATED CELL BIAS TEMPERATURE TEST RESULTS
MAXIMUM POWER OUTPUT Q-, R-, AND V-CELLS
(Test completed)

Cell	Temp C	Time (hr)	Total Cells	Range of Maximum Power Degradation 0-2%	3-9%	10-19%	20-29%	30-49%	50-100%
Q	75	600	25	2	23				
		1200	25					2	23
		2400	24					2	22
		4800	24					1	23
Q	135	600	20		1	16	3		
		1200	20			12	7	1	
		2400	20				2		18
		4800	20				1	1	18
Q	150	300	20		2	12	6		
		600	20			5	10	4	1
		1200	20						20
		2400	20						20
R	75	600	20	13	7				
		1200	15	10	5				
		2400	10	5	5				
		4800	20	9	2	3		4	2
R	135	600	16	10	6				
		1200	16	11	5				
		2400	14	4	8	2			
		4800	15	9	3	2	1		
R	150		test not run because of lack of samples						
V	75	600	23	21	2				
		1200	15	3	11	1			
		2400	interpretation difficult because of mechanical defects						
		4800	18	2	4	7	1	2	2
V	135	600	17	17					
		1200	17	14	3				
		2400	15	9	6				
		4800	16	4	3	6	2	1	
V	150	300	20	18	2				
		600	16	15	1				
		1200	14	7	7				
		2400	interpretation difficult because of mechanical defects						

TABLE 3C
UNENCAPSULATED CELL BIAS TEMPERATURE TEST RESULTS
MAXIMUM POWER OUTPUT W-, AND X-CELLS
(Test completed)

Cell	Temp C	Time (hr)	Total Cells	Range of Maximum Power Degradation 0-2%	3-9%	10-19%	20-29%	30-49%	50-100%
W	75	600	25	24	1				
		1200	25	6	19				
		2400	25	7	18				
		4800	25	3	22				
W	135	600	20	15	5				
		1200	20	17	3				
		2400	20	8	12				
		4800	19	8	11				
W	150	300	20	17	3				
		600	20	17	3				
		1200	20	4	15	1			
		2400	20	1	15	4			
X	75	600	25	25					
		1200	25	24	1				
		2400	25	22	3				
		4800	25	23	2				
X	135	600	interpretation difficult because of mechanical defects						
		1200	interpretation difficult because of mechanical defects						
		2400	20		4	8	1	5	2
		4800	20			7	4	5	4
X	150	300	interpretation difficult because of mechanical defects						
		600	interpretation difficult because of mechanical defects						
		1200	test discontinued because of mechanical defects						
		2400	test discontinued because of mechanical defects						

TABLE 3D
UNENCAPSULATED CELL BIAS TEMPERATURE TEST RESULTS
MAXIMUM POWER OUTPUT Y- AND Z-CELLS
(Test completed)

Cell	Temp C	Time (hr)	Total Cells	Range of Maximum Power Degradation 0-2%	3-9%	10-19%	20-29%	30-49%	50-100%
Y	75	600	25	-9	-15				
				+1					
		1200	25	-10	-13				
				+1	+1				
		2400	25	-8	-13				
				+3	+1				
		4800	25	-2	-15	-2			
				+4	+2				
Y	135	600	20		-10	-9	-1		
		1200	20		-10	-9	-1		
		2400	20	-2	-9	-9			
		4800	20	-2	-1				
				+3	+3	+7	+2	+2	
Y	150	300	20		-10	-10			
		600	20		-9	-10	-1		
		1200	20	-1	-7	-4			
					+8				
		2400	20		-1				
				+1	+2	+7	+7	+2	
Z	75	600	19	8	11				
		1200	15	10	5				
		2400	16	1	14	1			
		4800	15	15					
Z	135	600	16	16					
		1200	15	11		4			
		2400	15	12	3				
		4800	15	14		1			
Z	150	300		data unavailable					
		600	17	11	6				
		1200	16	7	6	3			
		2400	16	5	5	5	1		

NOTE: All values are positive unless otherwise noted.
A negative value of degradation is an improvement.

TABLE 4
UNENCAPSULATED CELL BIAS-TEMPERATURE TEST RESULTS
CATASTROPHIC MECHANICAL CHANGE
(tests completed)

Cell	Temp	Total # in test	Defect Category -- M=moderate, S=severe							
			Leads		Fracture		Grid		Back	
			M	S	M	S	M	S	M	S
N	75	25	1			1	20		20	
N	135	19		2		4				
N	150	20		2			10		10	
O	75	25				1	5		4	
O	135	20			2				2	
O	150	20	9			3	7		3	
P	75	25	13		3	1	5		3	
P	135	20	3		2		1		1	
P	150	20	2		2		11		10	
Q	75	25	4	1	4	1	11		11	
Q	135	20	1		5				1	
Q	150	20	3		1		14			
R	75	25	18		11	2	7		24	
R	135	20	12	1	7	12	3	1	7	3
R	150		test not run because of lack of samples							
V	75	25			1	10	3		7	
V	135	20			3	5	1		1	
V	150	20			3	7	1		2	
W	75	25					1			
W	135	20			2	1	4			
W	150	20					4		18	
X	75	25					9		8	
X	135	20	2				20		20	
X	150	20	4	15			11	6	9	
Y	75	25	1				25			
Y	135	20	4		2					
Y	150	20	5		2		2			
Z	75	25			1	7				
Z	135	20	4		1	5				
Z	150	18	10		2	4	13			

TABLE 5
UNENCAPSULATED CELL 85 C/85% RH TEST RESULTS
MAXIMUM POWER OUTPUT DEGRADATION
(test completed)

Cell	Time (hr)	Total Cells	Range of Maximum Power Degradation 0-2%	3-9%	10-19%	20-29%	30-49%	50-100%
N	250	15	-1					
			+3	+8	+2			
	500	15	-2					
			+2	+6	+3	+2		
	1000	15	-2					
			+1	+7	+3	+1		
	2000	13	-2					
				+7	+2	+1		
O	250	14	-2					
			+12					
	500	14	-2					
			+9	+3				
	1000	14	-1					
			+5	+8				
	2000	14	-1					
			+4	+9				
P	250	15	-3	-7				
			+3	+2				
	500	15	-2	-1				
			+4	+5	+3			
	1000	15	-1	-2				
			+2	+7	+2			
	2000	14	-2	-1				
			+5	+5	+1			
Q	250	15	+1	+11	+2			
	500	15		+10	+5			
	1000	14		+2	+12			
	2000	10			+9	+1		
R			test not run because of lack of samples					
V	250	15	-5					
			+8	+1	+1			
	500	14	-5	-1				
			+5	+2		+1		
	1000	14	-3	-1				
			+7		+1	+2		
	2000	14	+11	+1		+2		

TABLE 5 (continued)

W	250	15	+10	+5
	500	15	+11	+4
	1000	15	+1	+14
	2000	15	+2	+13
X	250	15	+10	+5
	500	14	+8	+6
	1000	13	+11	+2
	2000	14	+7	+7
Y				
Z				

Note: All values are positive unless otherwise noted.
A negative value of degradation is an improvement.

TABLE 6
UNENCAPSULATED CELL 85 C/85% RH TEST RESULTS
CATASTROPHIC MECHANICAL CHANGE
(tests completed)

Cell	Total # in test	Defect Category -- M=moderate, S=severe							
		Leads		Fracture		Grid		Back	
		M	S	M	S	M	S	M	S
N	15	3		1		13			
O	15			1		7			
P	15	3		3					
Q	15				1	3			
R		test not run because of lack of samples							
V	15			2	2	14		5	
W	15								
X	15	1				5			
Y	15								
Z		cells not tested							

TABLE 7
UNENCAPSULATED CELL PRESSURE COOKER TEST RESULTS
MAXIMUM POWER OUTPUT DEGRADATION
(tests completed)

Cell	Time (hr)	Total Cells	Range of Maximum Power Degradation 0-2%	3-9%	10-19%	20-29%	30-49%	50-100%
N	50	8	6	2				
	100	6	4	2				
	200	8	1	3	1		1	2
	500	8	2	1	2		1	2
O	50	10	4	3	3			
	100	10		5	4	1		
	200	10		5	1	3		1
	500	10		2	3	4	1	
P	50	10			5	5		
	100	8			4	4		
	200	(test stopped due to operator error)						
	500							
Q	50	10	3	6	1			
	100	10	1	6	3			
	200	10	1	3	3	1	1	1
	500	9		1	4	1	2	1
R		test not run because of lack of samples						
V	50	10	8	1	1			
	100	10	6	2	2			
	200	10	1	6		3		
	500	10		1	4	4	1	
W	50	10	4	4	2			
	100	10	4	4	2			
	200	10	1	5	1	2	1	
	500	8	4	4				

TABLE 7 (continued)
UNENCAPSULATED CELL PRESSURE COOKER TEST RESULTS
MAXIMUM POWER OUTPUT DEGRADATION

Cell	Time (hr)	Total Cells	Range of Maximum Power Degradation 0-2%	3-9%	10-19%	20-29%	30-49%	50-100%
X	50		interpretation difficult because of mechanical defects					
	100		interpretation difficult because of mechanical defects					
	200		interpretation difficult because ofmechanical defects					
	500		test terminated because of mechanical defects					
Y	50	10				2*	8*	
	100	10					10*	
	200	10				2*	8*	
	500	10	10					
Z	50	8	8					
	100	8	8					
	200	8			2	5		1
	500	8						8

*NOTE: Y-cell Pm values represent increases rather than decreases!

TABLE 8
UNENCAPSULATED CELL PRESSURE COOKER TEST RESULTS
CATASTROPHIC MECHANICAL CHANGE

Cell	Total # in test	Defect Category -- M=moderate, S=severe							
		Leads		Fracture		Grid		Back	
		M	S	M	S	M	S	M	S
N	10	1	2			5		3	
O	10			1		7		10	
P	operator error required premature termination of test								
Q	10	2							
R	test not run because of lack of samples								
V	10			1		1			
W	10								
X	10	2	7			2	8	10	
Y	10	3							
Z	10	4							

TABLE 9
SUMMARY OF UNENCAPSULATED CRYSTALLINE CELL ACCELERATED TEST RESULTS

Cell	B-T Tests	PC Tests	TC/TS	Comments
N	average	average	poor	
O	poor	average	average	
P	good	poor	good	
Q	very poor	poor	poor	Back contact Schottky formation
R	poor	--	--	Fracture during handling
V	average	average	poor	
W	good	average	poor	
X	very poor	very poor	very poor	Loss of grid adhesion
Y	poor	very poor	poor	Increase in Pm
Z	average	very poor	--	Fracture

2.3 Outdoor Real-Time Testing of Individual Cells

The outdoor test rack was installed in an effort to see if a relationship could be established between real time testing and accelerated testing. The real-time test program has been in operation approximately one year during which considerable experience has been gained in outdoor test procedures. It was found that the cells were exposed to liquid water in the form of rain and this constituted a stress quite unlike any in the laboratory. In addition, a number of hail storms and one freak snow caused some mechanical fracturing of the unencapsulated cells. To avoid these effects the original rack has been protected by the installation of a polycarbonate cover which permits free circulation of air over the cells, but avoids the problem of liquid water in contact with the cell surface and at the same time offers protection from hail. Figure 6 is a photograph of the rack with its newly installed cover. The original cells were also replaced when the cover was added.

Table 10 shows the results obtained on the initial group of unencapsulated cells. It can be seen that several cells experienced large amounts of degradation. In general this was due to mechanical damage induced (we believe) as a result of water standing on the cells: one of the E-cell leads came unattached, the N- and X-cells lost a major portion of their grids, and the P-cell's lead, which was bonded at several points across the cell, lost contact at many of these points. The temperature at the back of the cells was measured at solar noon on a number of days and typically found to range from 30 to 40 C.

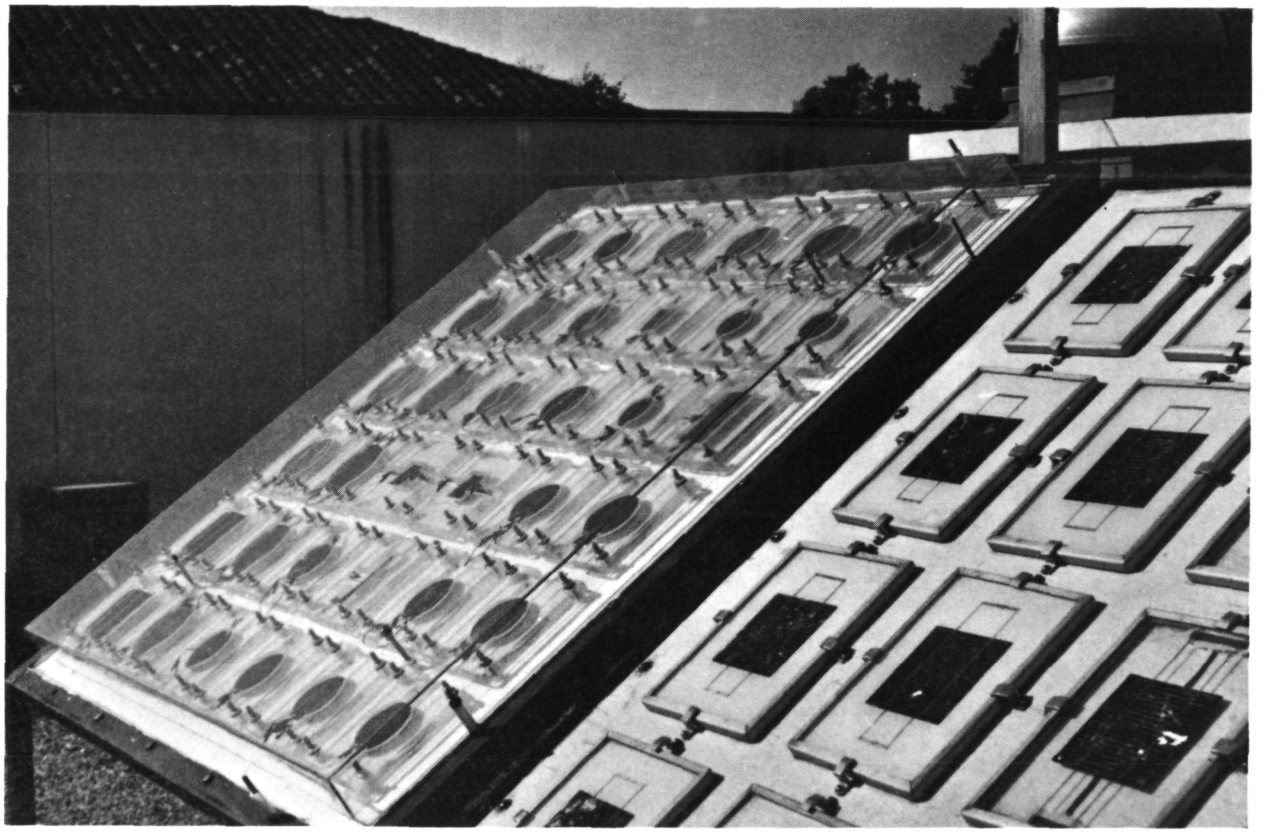

Figure 6. Photograph of Outdoor Real Time Test Rack

The encapsulated cells that were subjected to outdoor testing degraded very rapidly at first and then leveled off as can be seen from the data of Table 10. This may be a real effect or it may be an artifact of the measurement system. Further measurements may indicate which.

TABLE 10

UNENCAPSULATED CELL REAL-TIME TEST RESULTS
MAXIMUM POWER DEGRADATION

Cell Type	Approx Time (hours)	Total Cells	Range of Maximum Power Degradation				
			0-2%	3-9%	10-19%	20-29%	30-49%	50-100%
B	7200	1		1				
C	7300	2	1	1				
F	7300	1		1				
E	8500	1						1
M	7300	1	1					
N	8900	3					1	2
O	8600	2		1	1			
P	7300	1						1
Q	7300	2	1	1				
W	7300	2		1	1			
X	8800	1						1

3.0 a:Si RELIABILITY INSTRUMENTATION RESEARCH

3.1 General Considerations

The ability to make repeatable electrical measurements days, weeks, and months apart is essential to an accelerated test program. The greater the repeatability of the measurement instrumentation the smaller the changes which can be detected, and consequently the shorter the required acceleration time. Under the Clemson JPL contract, a short interval measurement system was developed for the electrical characterization of crystalline cells up to 4 inches in diameter. This instrumentation, which has been continually improved and upgraded over the past 4 years, has proven in practice to be repeatable to within 1%. Unfortunately, however, it cannot be used directly for a:Si cells with this same degree of repeatability. The major difficulty involves reproducibly setting the illumination levels over extended periods.

Reference cells have been traditionally used to adjust laboratory simulator illumination levels to give an intensity of 1-sun. In crystalline cell measurements the reference cell is made from a portion of a cell of the same type as that undergoing testing and is calibrated against natural solar radiation by a standards group at an organization such as JPL using straightforward, but often tedious techniques. Accelerated reliability testing, as opposed to efficiency measurement, does not require that the illumination level be exactly 1-sun, but only that it be approximately 1-sun. It is necessary, however, that it be repeatable. In practice, a complete cell of the type undergoing measurement is measured at this 1-sun level (the

complete IV curve is taken) and set aside to be used as a standard cell whenever it is necessary to initialize illumination levels. Unfortunately, when working with a:Si cells it is neither possible to calibrate a reference cell or utilize a standard cell, as is the case for crystalline cells, because the output of a:Si cells is not necessarily stable. The output of an a:Si cell may depend on its illumination history and other factors. Nor is it possible to use a stable crystalline cell directly as a standard because crystalline silicon and a:Si have different spectral sensitivities. a:Si cells are more sensitive in the blue (uv) region of the spectrum than are crystalline silicon cells. It is known that the ELH lamps which are used in the short interval light source have excellent short term stability, but change their spectral characteristics over their complete 48 hour life. Thus as ELH simulator bulbs age and are replaced it would be possible to obtain two identical intensity readings with a standard crystalline cell, but which would appear markedly different if viewed by an a:Si cell.

A secondary consideration regarding illumination is the larger dimension of many a:Si cells. Crystalline cells occupy areas normally not exceeding 4-inches x 4-inches, but a:Si submodules, which are collections of cells monolithically interconnected on a common substrate or superstrate, may have dimensions of up to 1-foot square with the individual cells having one dimension as great as that of the submodule edge. Thus it is necessary to consider an extended area light source. The Clemson accelerated test program is primarily concerned with single a:Si cells rather than collections of interconnected cells and consequently is not as concerned with absolute uniformity over this extended area as with relative uniformity. In theory it should be possible to achieve relative uniformity by making sure that any

variation of illumination with distance remains constant and that the cell being measured is always geometrically positioned under the simulator in the same way. However, in actual practice it is probably as easy to insure absolute uniformity as relative uniformity and that is the approach that has bee taken in designing light sources for the a:Si accelerated test program.

Much of the hardware and software used to acquire IV characteristics with the crystalline short interval tester are directly applicable to a:Si measurement and although a completely new system has been constructed for a:Si cells it incorporates many of the proven concepts of the previous tester.

3.2 Simulated a:Si Standard Cell

In order to achieve the necessary repeatability for reliability testing it is absolutely essential to have a stable standard cell. Various approaches are being followed in a number of different laboratories to simulate the spectral characteristics of an a:Si cell using stable silicon cells. The particular approach currently being investigated at Clemson, and which was reported in some detail at the 24th Project Integration Meeting (PIM) in October 1984, involves using a number of individually filtered silicon photo diodes as illustrated in Figure 7. The output of each diode is connected to an op-amp and the op-amp outputs are mixed together in the right proportion to simulate an a:Si cell. The diodes, op-amps, and resistors are small and can be mounted together in a single thermal mass. To calibrate the simulated standard cell, the relative output of an a:Si cell, of the type to be measured, is first measured by exposing it through the set of filters. When doing this it is important to use a white light bias of approximately 1-sun in order to fill

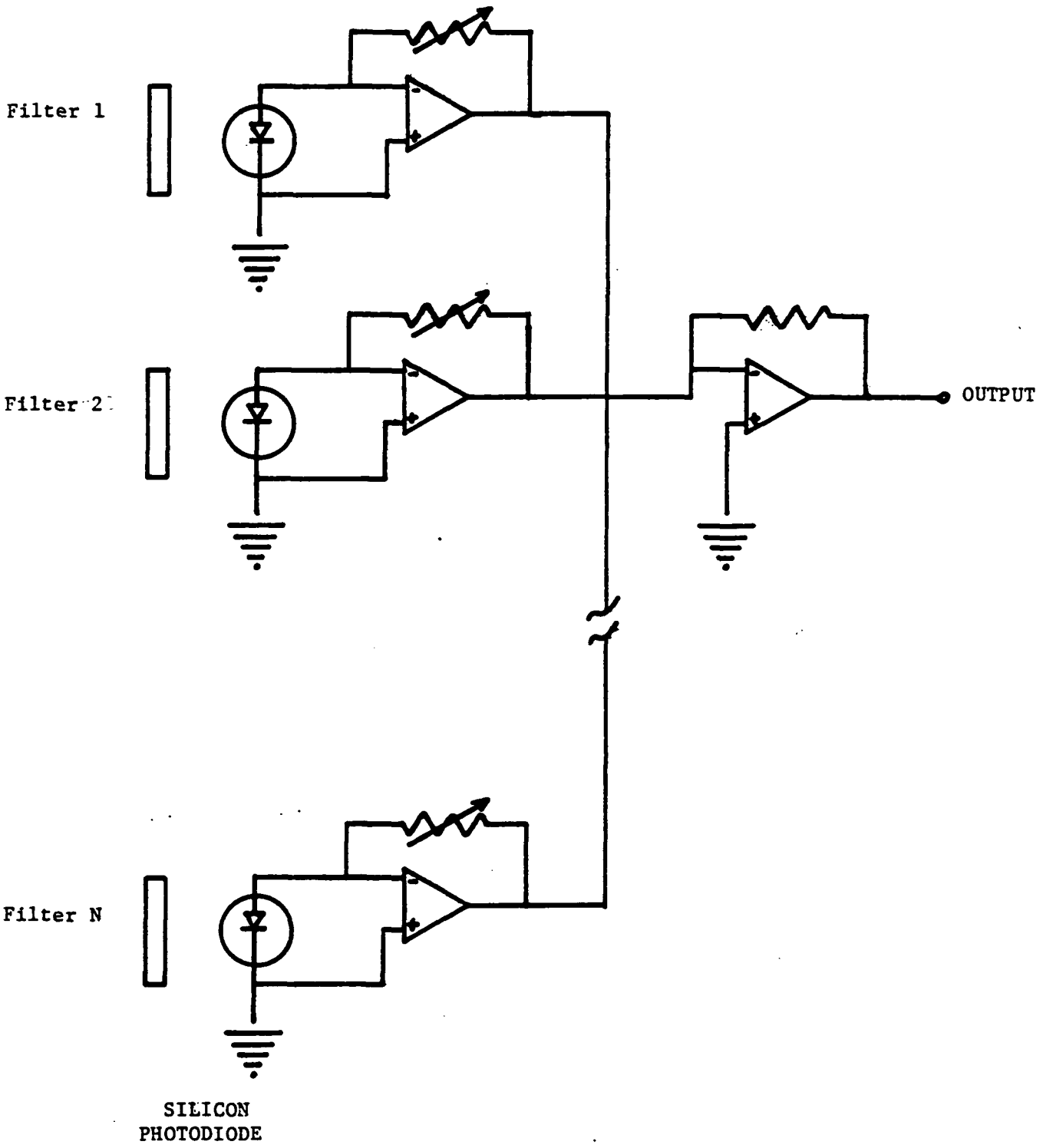

Figure 7. Approach to a Simulated a:Si Standard Cell Using Filtered Crystalline Silicon Photodiodes

the traps in the amorphous film. If this is not done the measured spectral sensitivity of the cell will be different from that which actually occurs under terrestrial conditions. This is accomplished by using a continuous (DC) white light and chopping (AC) the filtered light. An AC amplifier can then be used to determine the cell's response. Following this the resistors in the composite standard cell are adjusted so the output of each correspondingly filtered diode is in this same proportion. To achieve adequate sensitivity the light source used for the initial calibration should be rich in uv, such as natural sunlight. The resultant simulated cell should have great flexibility and allow the rapid simulation of nearly any type of construction. Such a cell for use in accelerated testing is under development and an evaluation of its performance will be given in the next annual report.

3.3 Large Area Light Source

Because of expense and stability considerations the approach being take toward a large area light source is that of a multiple ELH lamp array. In such an array it is necessary to individually adjust the intensity of each lamp in order to produce uniform illumination over the target area. It is possible to vary intensity by changing the distance of the lamp from the target or through the use of neutral density filters. These approaches would require cumbersome mechanical systems and, in the case of the filters, would not necessarily produce a continuously variable output. Adjusting lamp voltages is the most simple method of intensity variation, although it has the undesirable effect of changing the spectral characteristics of the lamp by varying the filament temperature. Under normal conditions, however, these spectral changes are small if the voltage variation is kept within +10%, and any errors are

expected to be corrected by using a standard cell during initial setup.

Tungsten filament ELH lamps were chosen because, although their spectral characteristics are not optimum, they have the advantage of being stable, low cost, do not require ballasts, and can be operated from either the AC line or a DC supply. In order to determine the most efficient lamp arrangement a computer simulation was used to model the lamp characteristics. Data for this model was obtained by recording the intensity variation of several lamps over an eight inch square area. The lamps were free standing, not in a reflective barrel, and the distance from the lamp to the target was adjusted from 17 to 25 inches. The data taken from four lamps was averaged to produce the intensity variation plot shown in Figure 8. Recognizing the familiar shape of the curve it was found that by choosing the appropriate values for the variance and mean the intensity variation curve of a single lamp could be mathematically represented by the normal distribution function of the form,

$$I = \frac{1}{\sqrt{2\pi}\sigma} \exp\left[-\frac{((x-\overline{X})^2 + (y-\overline{Y})^2}{2\sigma^2}\right]$$

where σ is the variance

$\overline{X}$ and $\overline{Y}$ are the means in the x and y directions.

Using this equation the intensity contribution of each lamp was obtained and added to produce the intensity variation plot of the entire array over a one square foot area as shown in Figure 9. The use of 11 lamps in a hexagonal array with 6 inch spacing between the lamps and 17 inches between the light source and target produced a fairly uniform pattern. Figure 10 is a diagram of

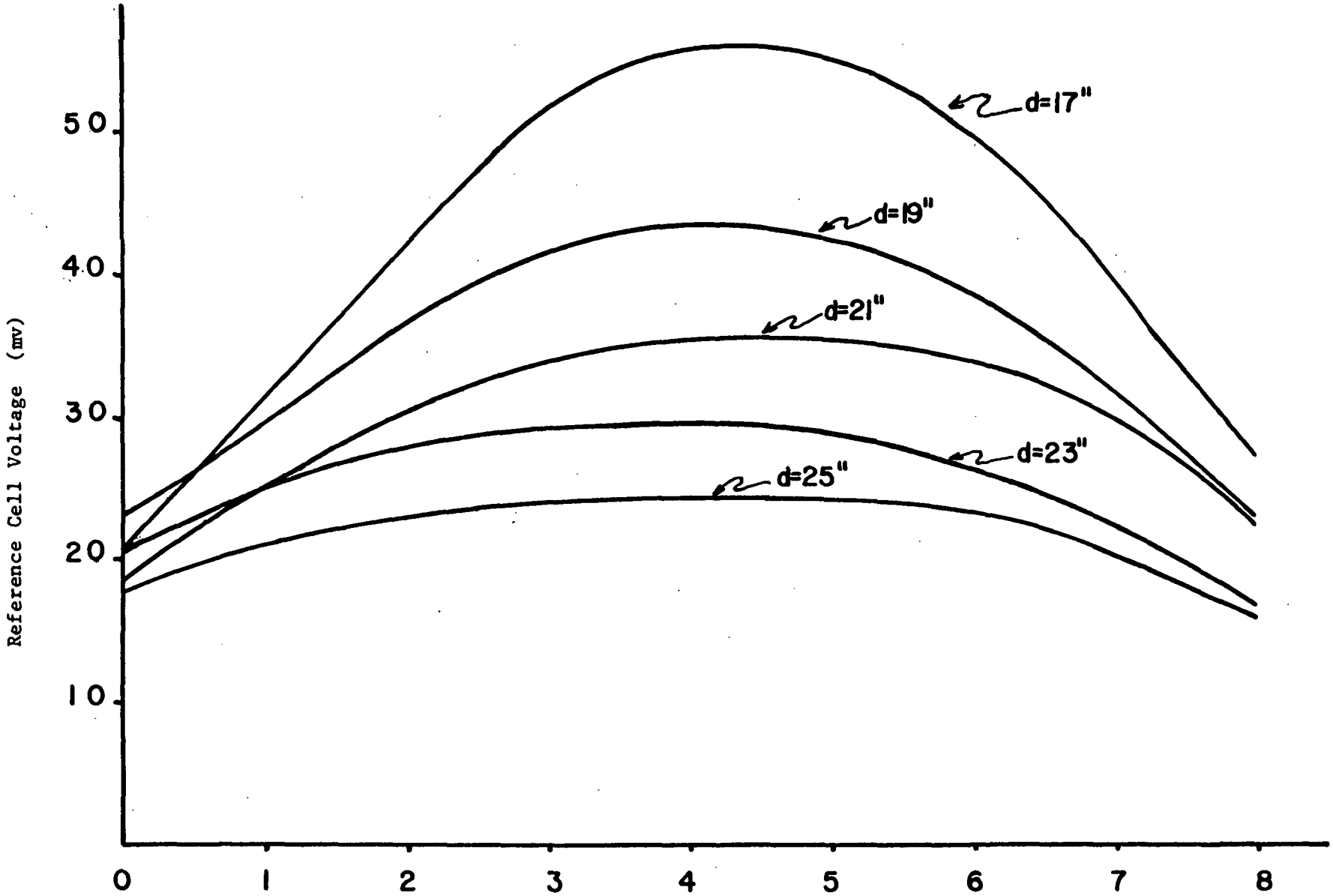

Figure 8. Average Measured Intensity Variation of ELH Lamps

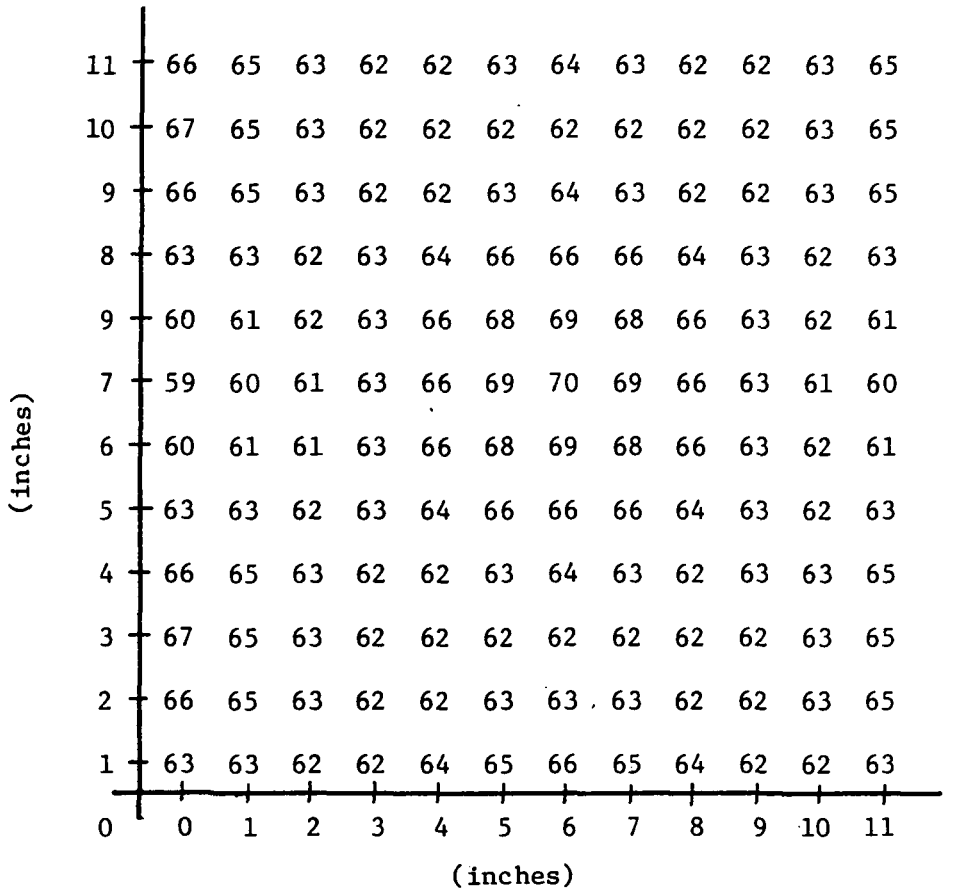

Figure 9. Calculated Intensities Over an Extended Area for An 11-Lamp ELH Array

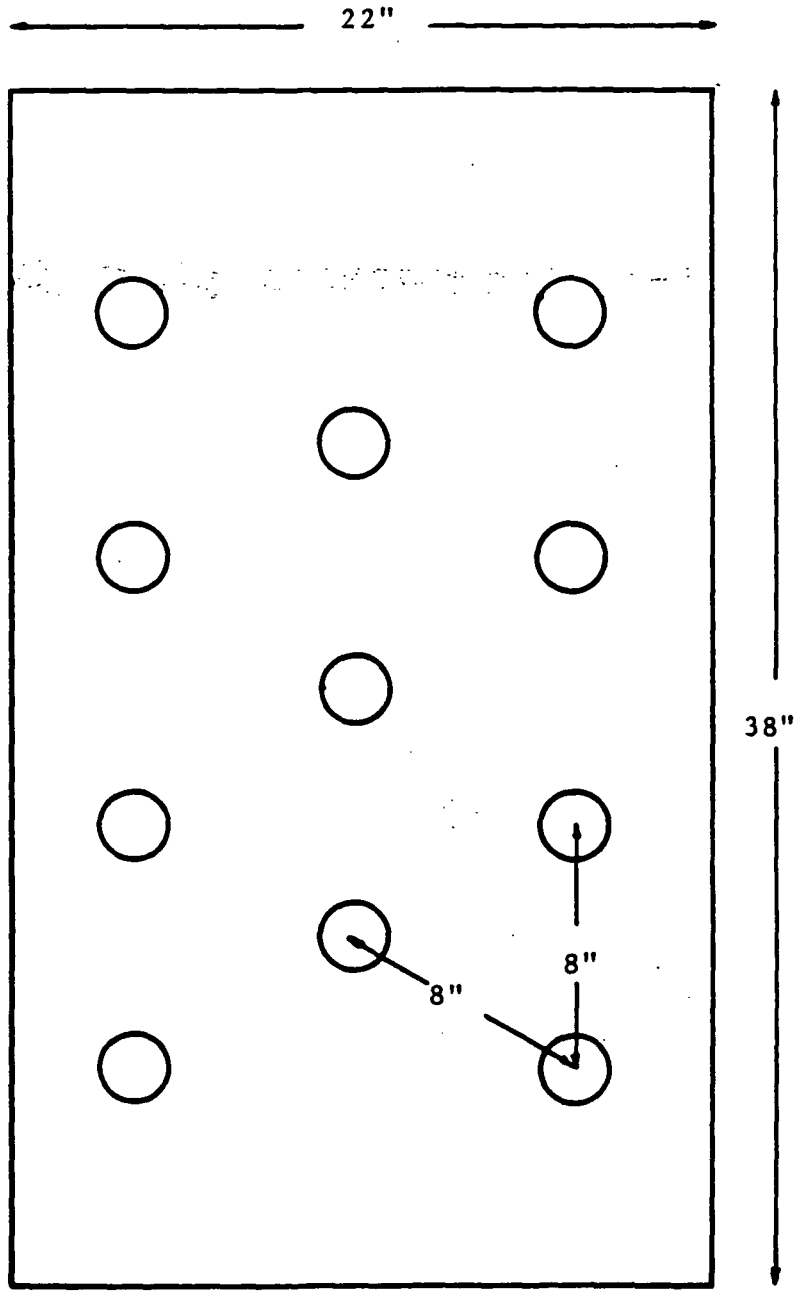

Figure 10. Lamp Location Diagram for 11-Lamp Array

the 11-lamp array. Each lamp is individually adjustable with regard to angle in order to correct for small manufacturing variations which may be present in the lamps. Measured values of the intensity variation over a one square foot target are given in Figure 11. Since the fabricated lamp assembly resulted in some high intensity spots, some further physical modifications were necessary in order to obtain a more uniform starting distribution from which the final distribution could be verniered through the use of small voltage excursions. Diffusers were of little help, but by independently tilting each lamp it was possible to achieve an initial variation which approached 10% as shown in the pattern of Figure 12.

Once the lamps' tilt angles are adjusted, it will be necessary to be able to individually vernier lamp voltages in such a way as to optimize illumination uniformity. It is of course not possible to discern intensity variations by eye so the approach that is under development is to use a 4x4 array of photodetectors. These photodetectors will in effect be multiple filtered diodes interconnected to form simulated standard cells as described in Section 3.2. The computer will use the output of the standard cells to construct an array of shapes whose position varies with intensity of the proper composition. Thus the display on the monitor will inform the operator as to the illumination uniformity and as to which Variacs must be adjusted for further improvement. Figure 13 is a schematic of the uniformity adjustment system.

With the simulated standard cell there will be no difficulty in setting the illumination level to its original value there is the possibility that a degradation mechanism might be present which would alter only a cell's blue

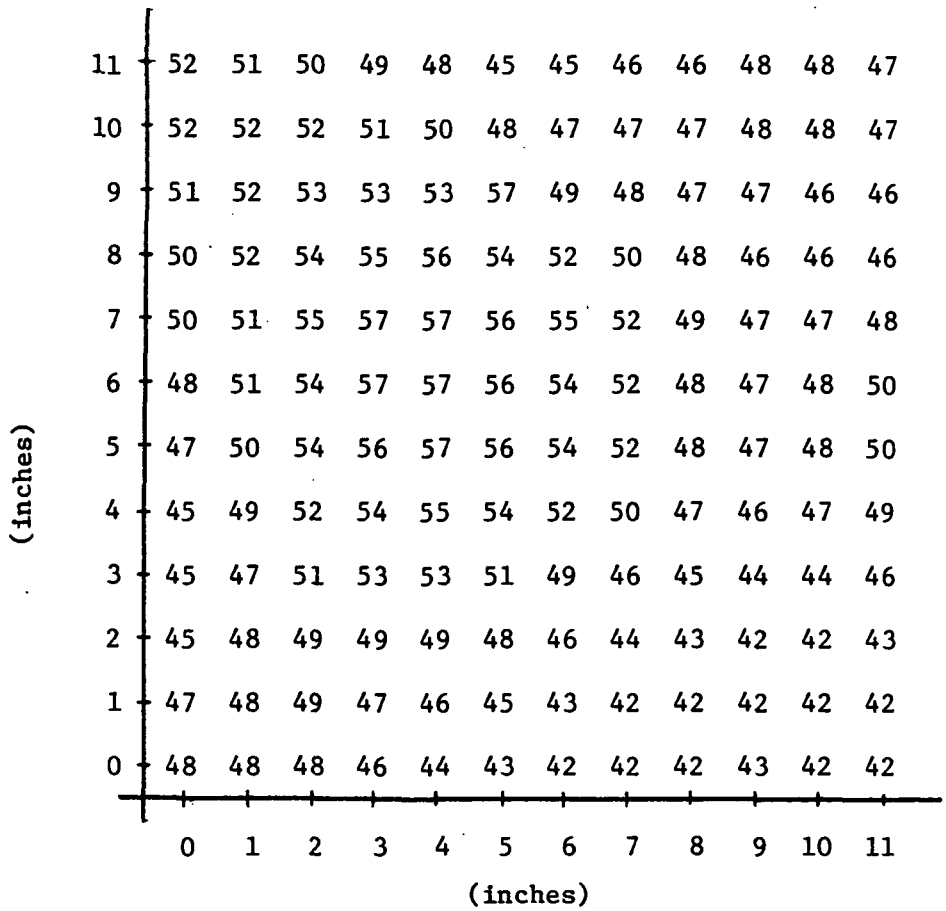

Figure 11. Original Measured Intensity Variation of 11-Lamp Array

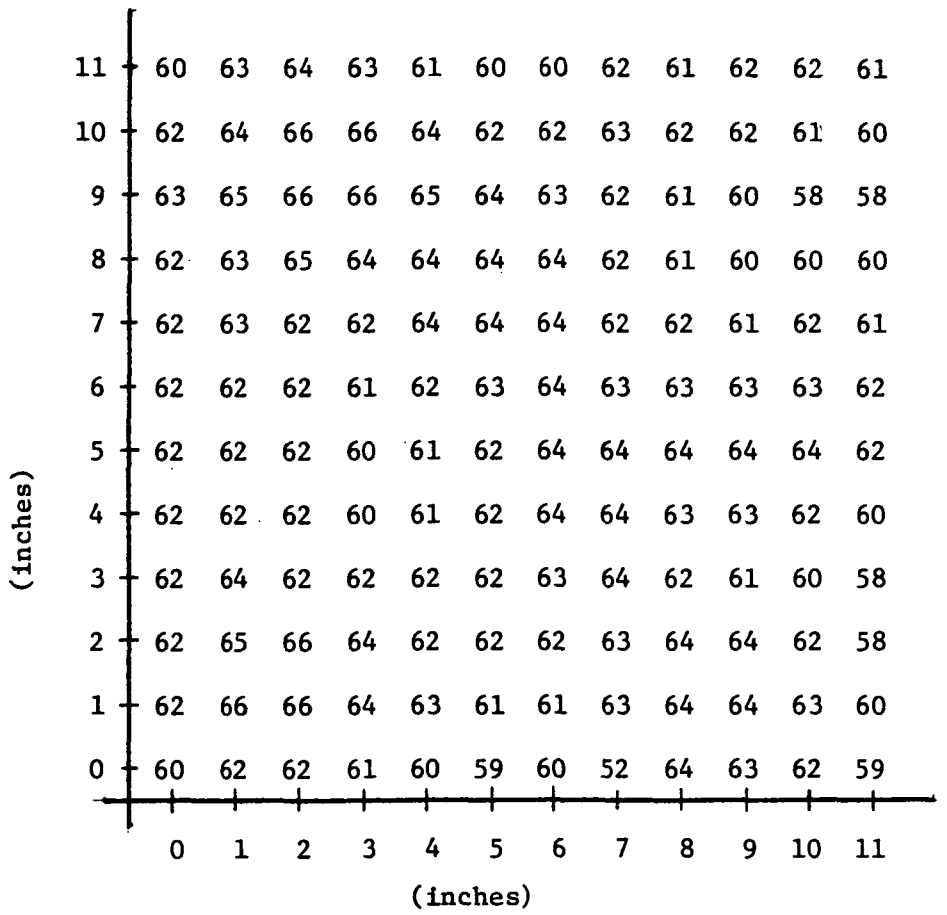

Figure 12. Measured Intensity Variation of 11-Lamp Array After Lamp Tilt Adjustment

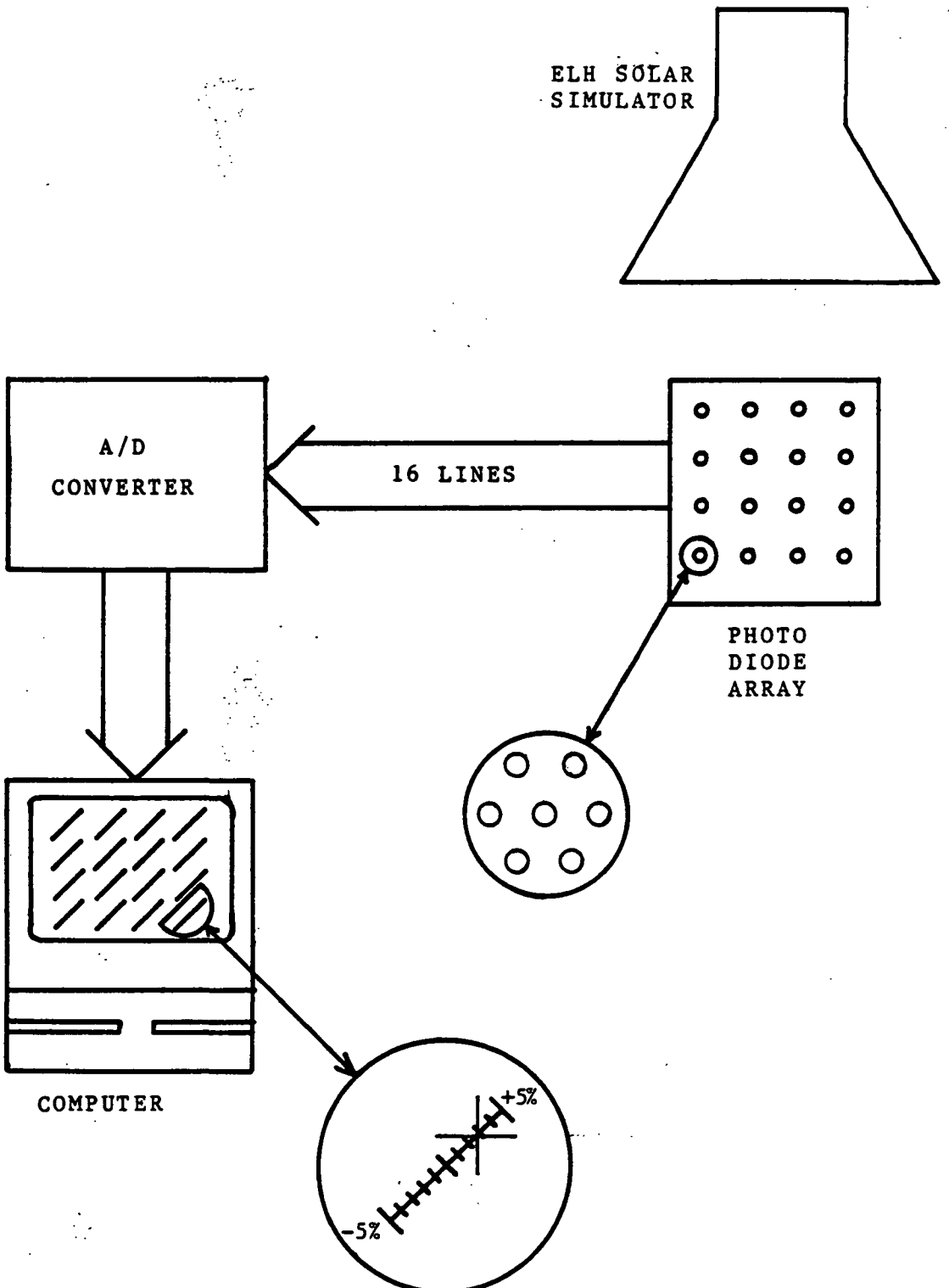

Figure 13. Intensity Monitoring and Adjustment System Schematic

response and since ELH lamps are relatively weak in the blue portion of the spectrum compared with natural sunlight, the full impact of this change might not be observed. It is felt that such selective degradation if present would be a second order effect. However, the possibility of enhancing the blue portion of the spectrum through the addition of a secondary light source is being investigated. A multi-vapor arc lamp appears to have suitable spectral characteristics as shown in Figure 14, although some filtering will be required to remove the peak at 600 nm.

3.4 System Configuration and Data Acquisition Procedures

A block diagram of the a:Si short interval tester is shown in Figure 15 and a photograph of the system in Figure 16. An IBM PC computer with two disk drives and graphics printer serves as controller for the instrumentation. The ELH lamps in the simulator may be powered by either adjustable DC supplies or by Variacs controlling the AC line voltage. If DC were to be used program operation would be similar to the crystalline silicon tester which uses 4 ELH lamps, each with its own power supply. With 11 lamps in the a:Si tester, however, the cost of power supplies (approximately $800 each) becomes excessive. Therefore a procedure has been developed to eliminate any illumination ripple by taking data only at the same point in the lamp's cycle. This is accomplished by sensing the light with a separate detector and using its output to trigger the acquisition of a data point when the illumination reaches the 1-sun condition. Figure 17 shows the flow diagram for the data taking routine and Figure 18 illustrates the timing diagram.

Both the cell under test and the detector are placed under the simulator,

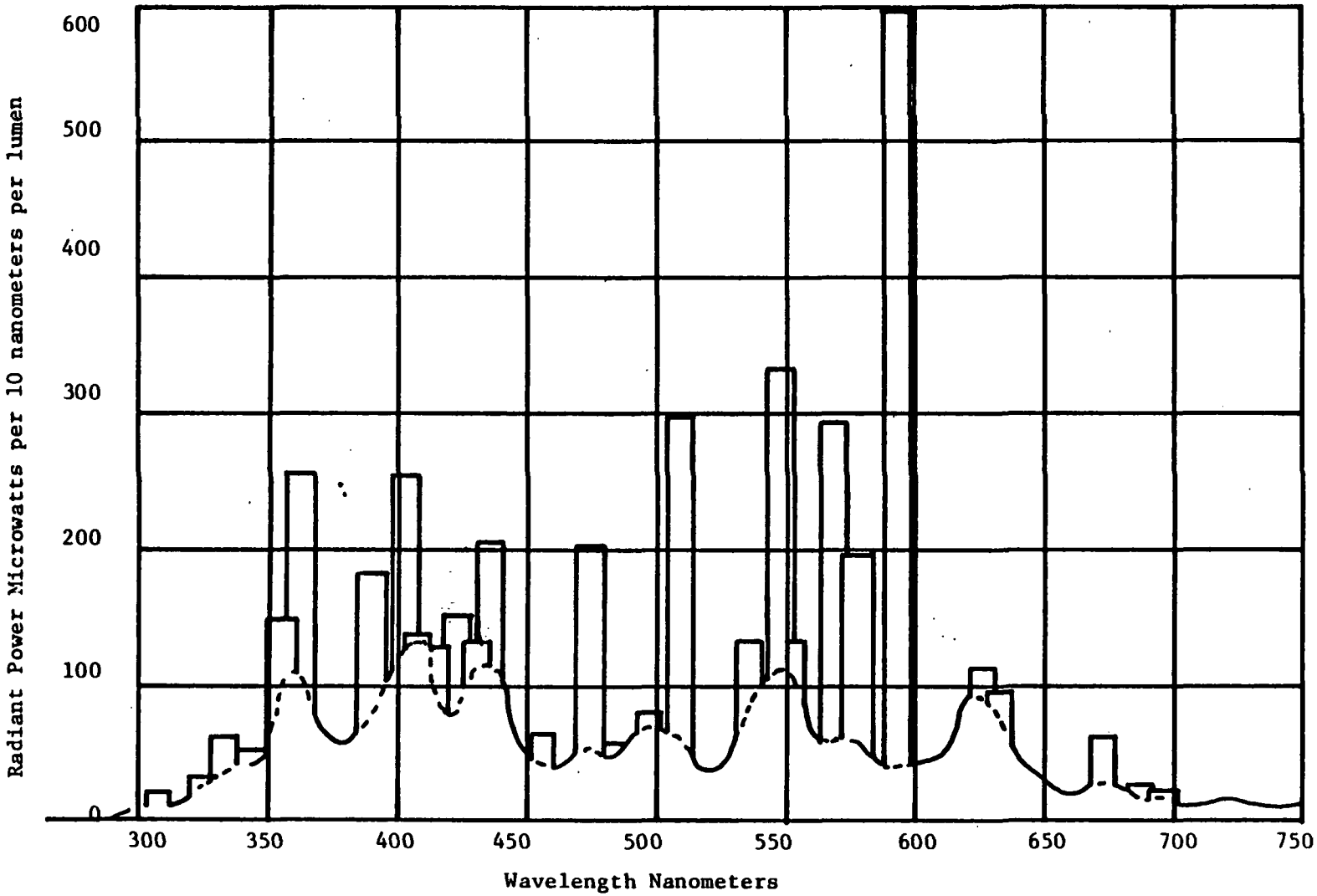

Figure 14. Multivapor Lamp Spectral Characteristics

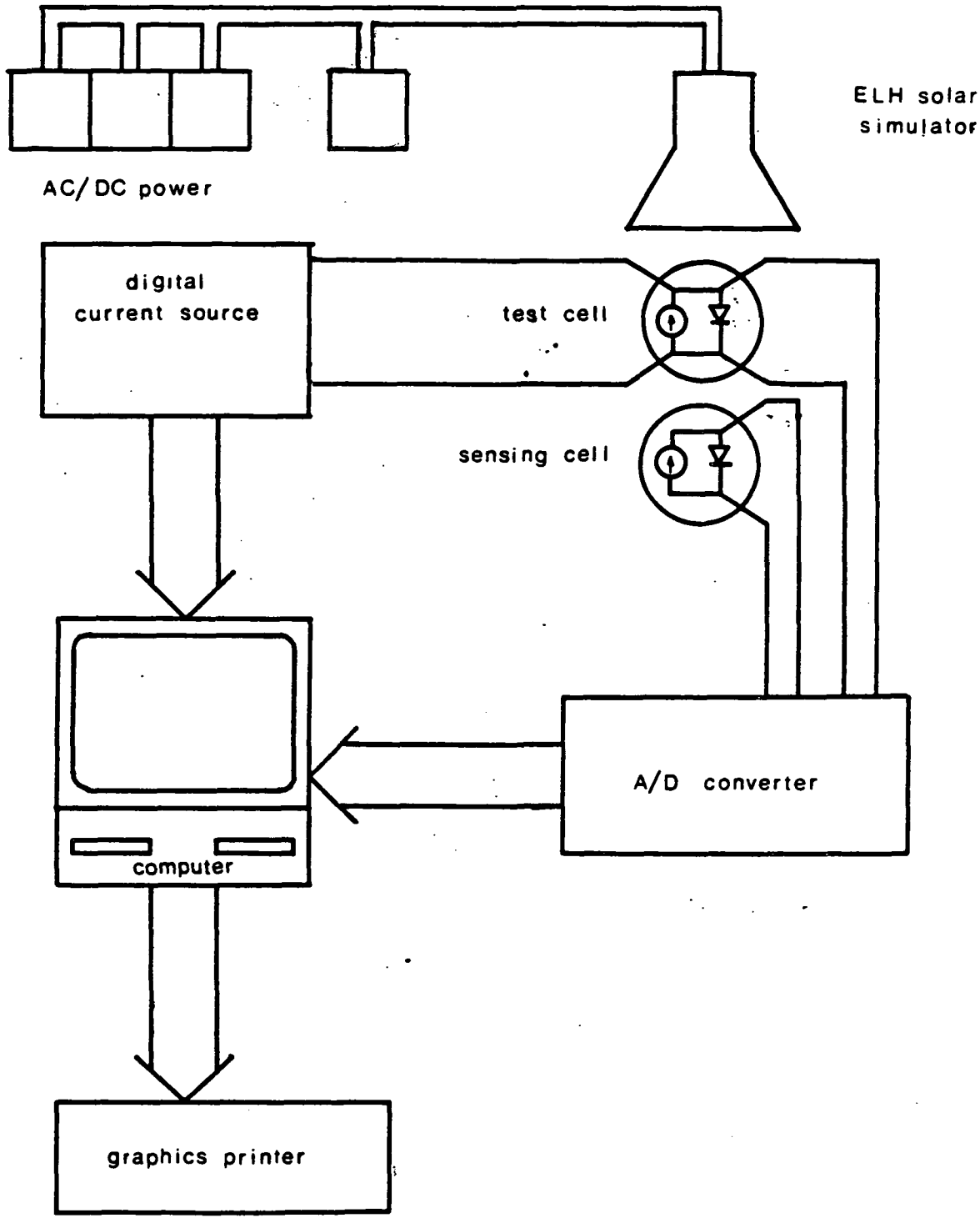

Figure 15. Block Diagram of the a:Si Short Interval Tester

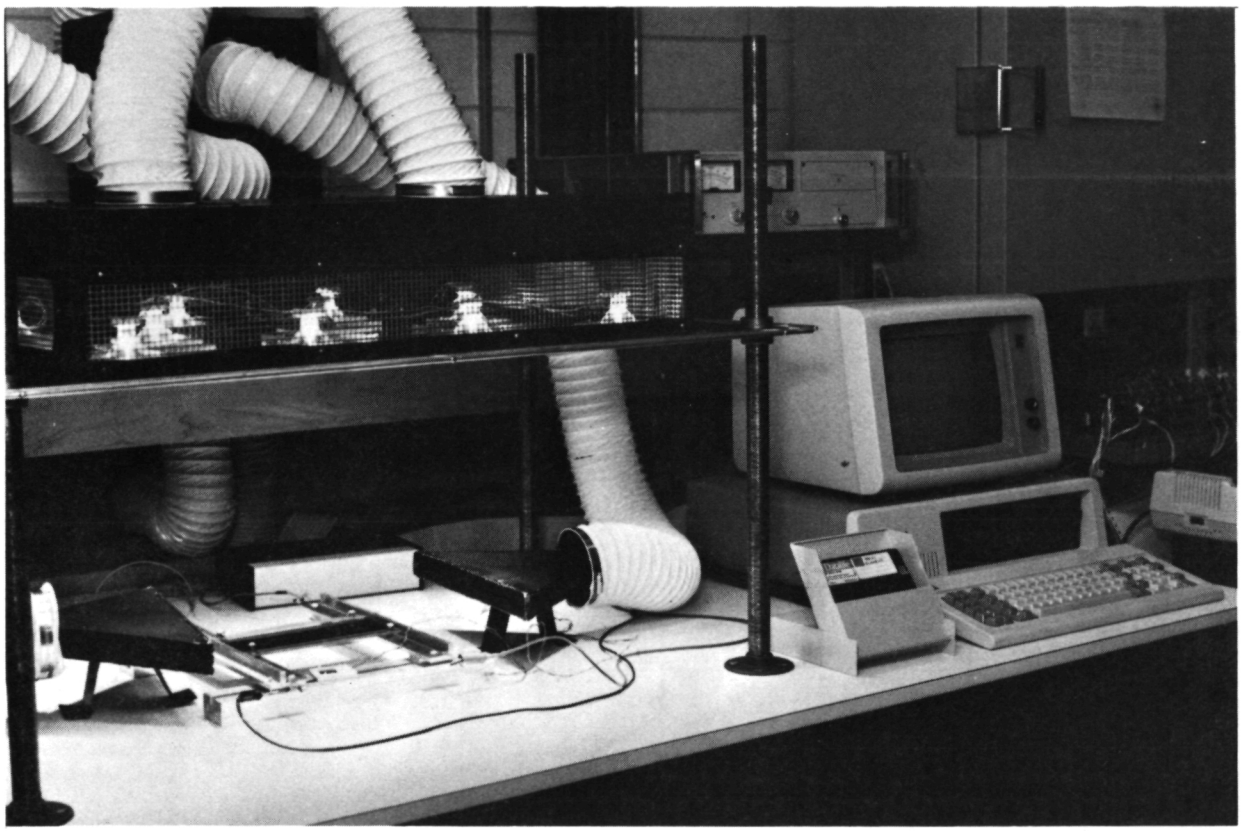

Figure 16. Photograph of the a:Si Short Interval Tester

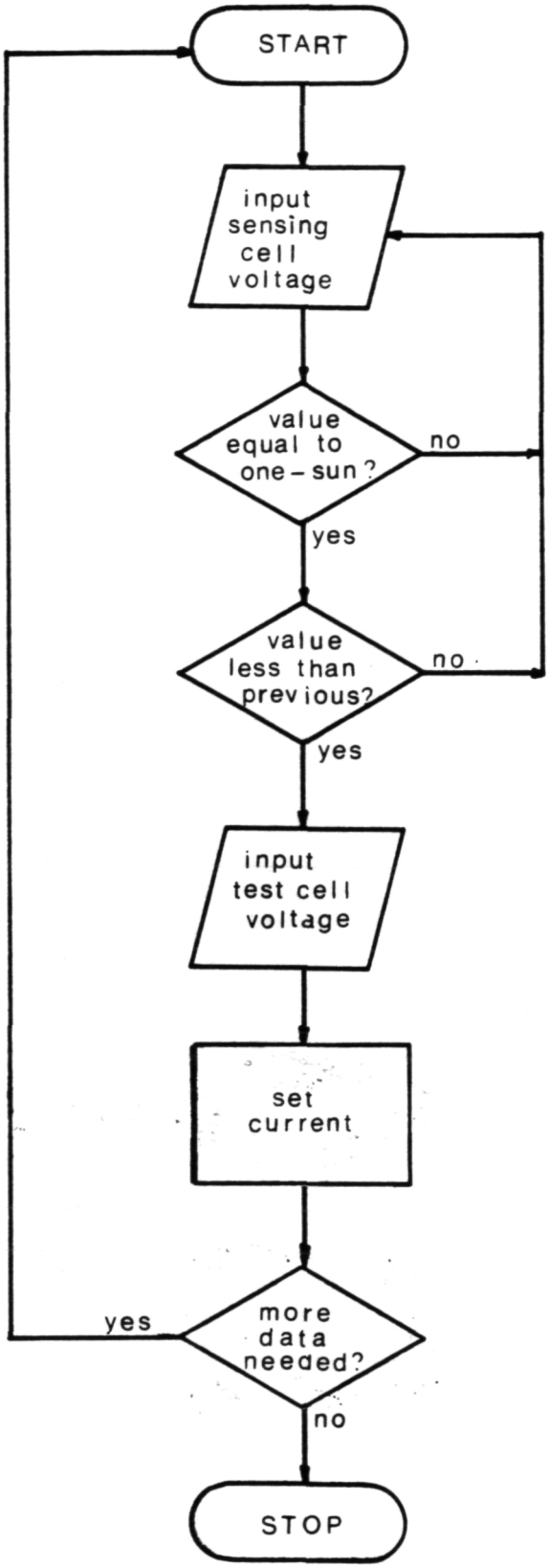

Figure 17. Flow Diagram of Data Taking Routine for AC Lamp Simulator

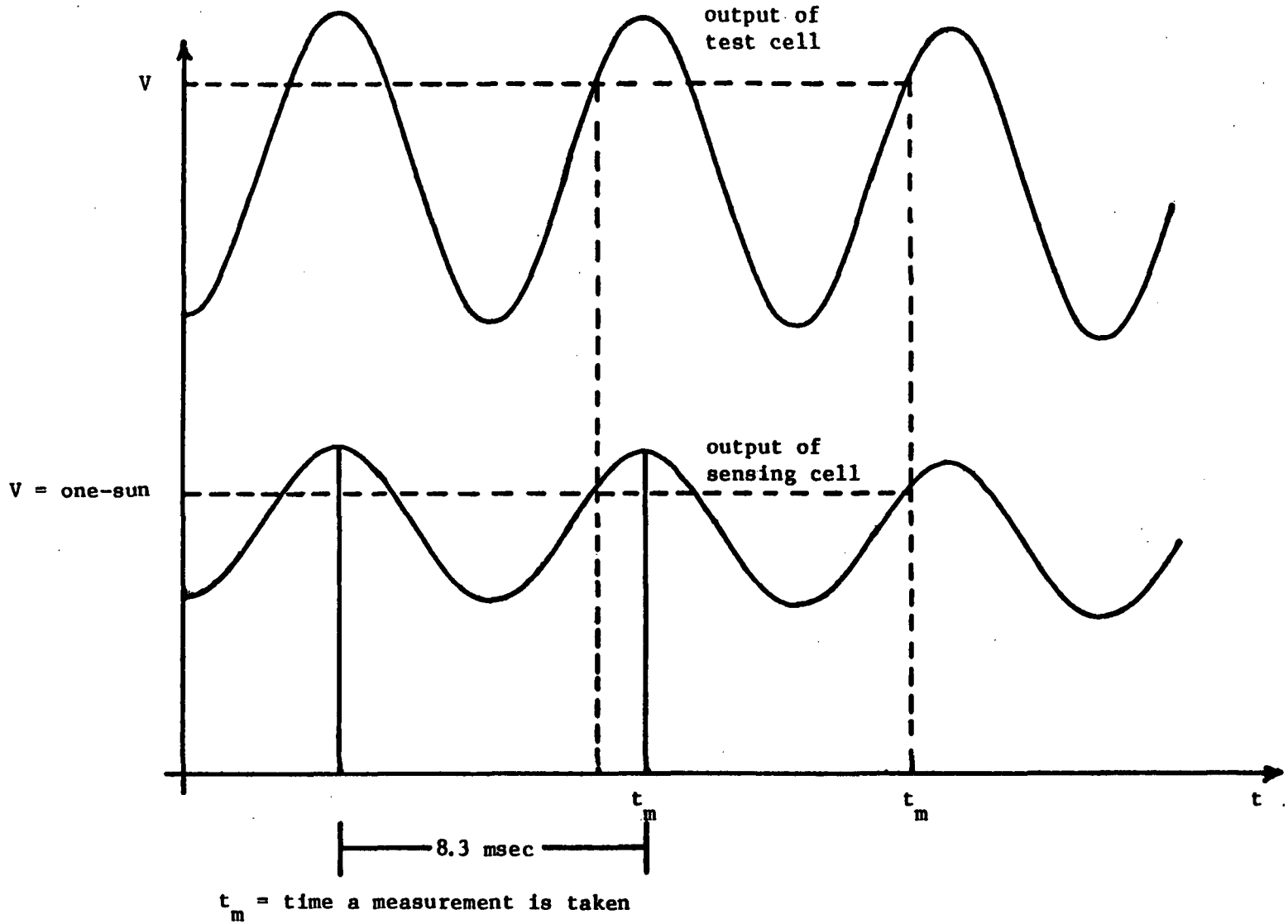

Figure 18. Timing Diagram of AC Light Source Data Acquisition Technique

with the detector being placed off-center since its operation does not depend on uniformity of illumination. The computer sets the programmable power supply to provide a particular value of current to the cell under test. The output of the detector is sampled at an approximately 20 kHz rate until a value is reached which corresponds to a 1-sun condition on the cell under test. When this occurs the voltage across the cell under test is acquired and stored in memory. The computer then advances the power supply to a new current setting and the process is repeated until the complete IV characteristic has been acquired. In order to check the accuracy of AC lamp operation against DC operation data was taken using both modes as shown in Figure 19. It can be seen that AC lamp control is able to produce quite uniform characteristics. Because the current supply is bipolar the a:Si short interval tester when completed will be able to obtain data in all three quadrants. It has been found in studying crystalline cells that taking data in the far-forward and reverse quadrants as well as the power quadrant is very helpful in determining degradation mechanisms.

3.5 Second and Fourth Quadrant Measurement

As reported in the Fourth Annual Report, it has become apparent that some degradation mechanisms may be more completely understood by studying the far-forward (and reverse) regions of the cell characteristic. It is possible to qualitatively observe these regions of the characteristic using a curve tracer, but for quantitative data it was necessary to modify the short interval tester. The procedure for this modification as applied to the crystalline tester is described in this section, with a similar procedure to be used for the a:Si tester.

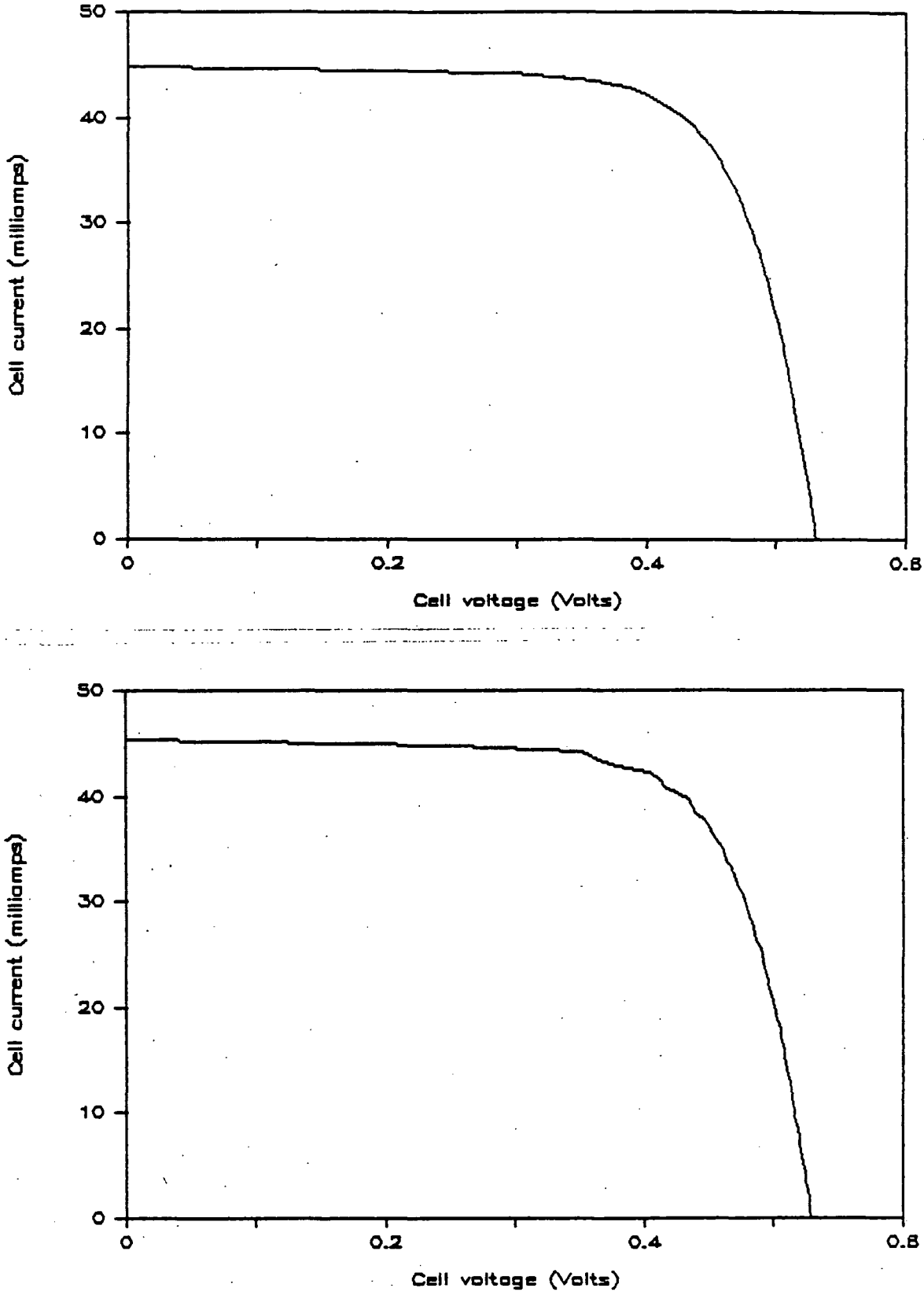

Figure 19. Comparison of AC (top) and DC (bottom) Data Collection Methods

Since the system A/D board was capable of converting both positive and negative voltages, taking data in the second (reverse) quadrant simply required a program change which caused the computer to increment the current past Isc. Data points are recorded until the voltage limit (1.25 volts) of the system is reached, the current limit (5 amperes) is reached, or the memory space (1024 data points) which has been set aside for storing second quadrant data is filled. The same number of data points are reserved in memory for each of the three quadrants.

Fourth (far-forward) quadrant measurements require the computer to set a negative value of current and to read the corresponding voltage through the A/D converter. Since the current supply for the crystalline short interval tester was unipolar (as contrasted with the a:Si supply which is bipolar) it was necessary to use a computer controlled relay to switch polarity. A diagram of this modification is shown in Figure 20. After all the data points are acquired and stored in in memory, the cell characteristic is displayed on the terminal, with all three quadrants being displayed in a single quadrant for best graphical resolution, as shown in Figure 21.

3.6 Low Temperature Measurement Jig for Crystalline Si Cells

Cell measurements are normally made at 28 C. The jigging arrangement for crystalline cells is such that both the front and back surfaces of the cell are exposed to a stream of conditioned air, i.e. the cell is not in contact with a heat sink, but quickly reaches the temperature of the air flowing over it. However, it is possible to obtain much useful information concerning

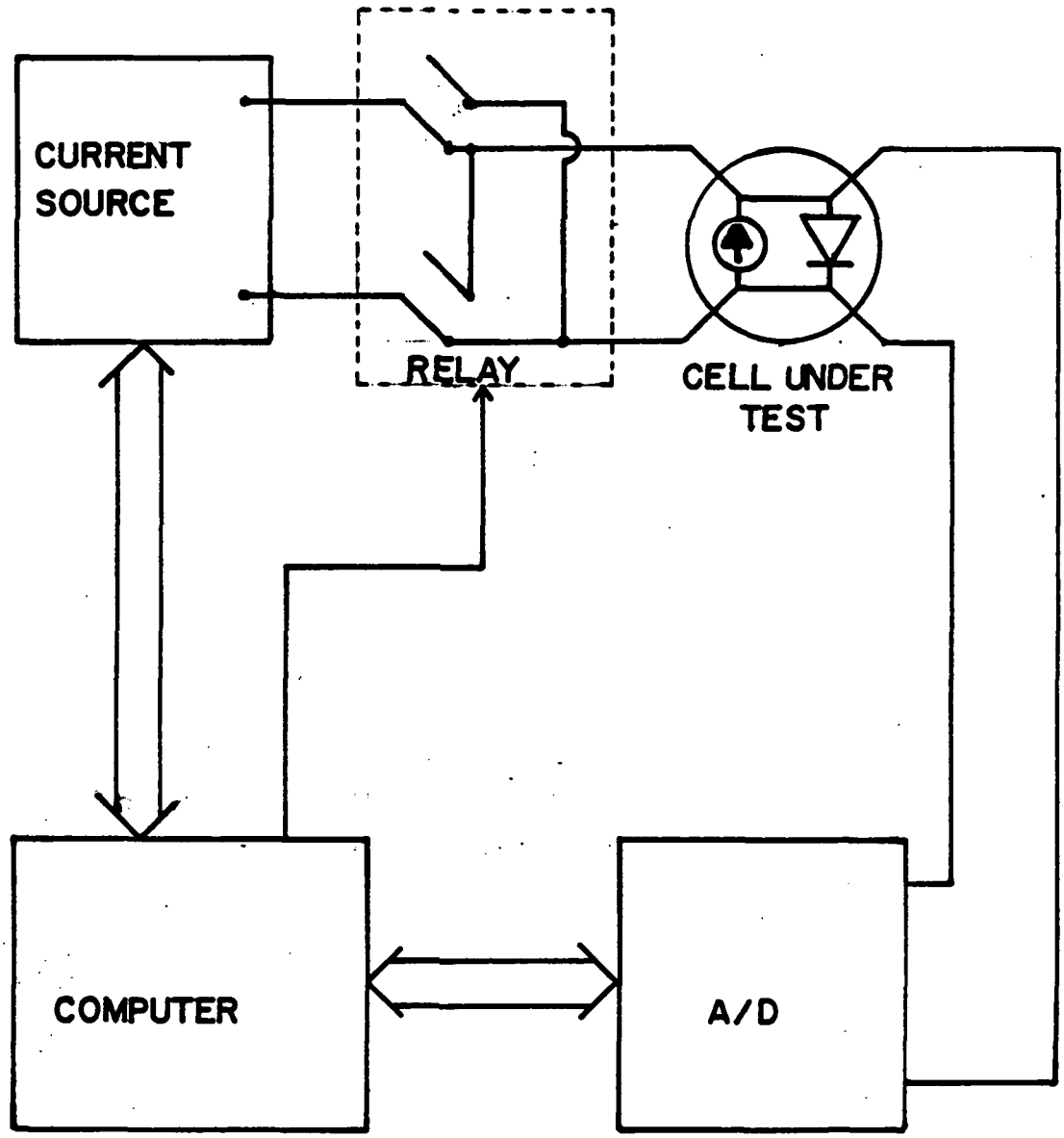

Figure 20. Power Supply Modification for 4th Quadrant Operation

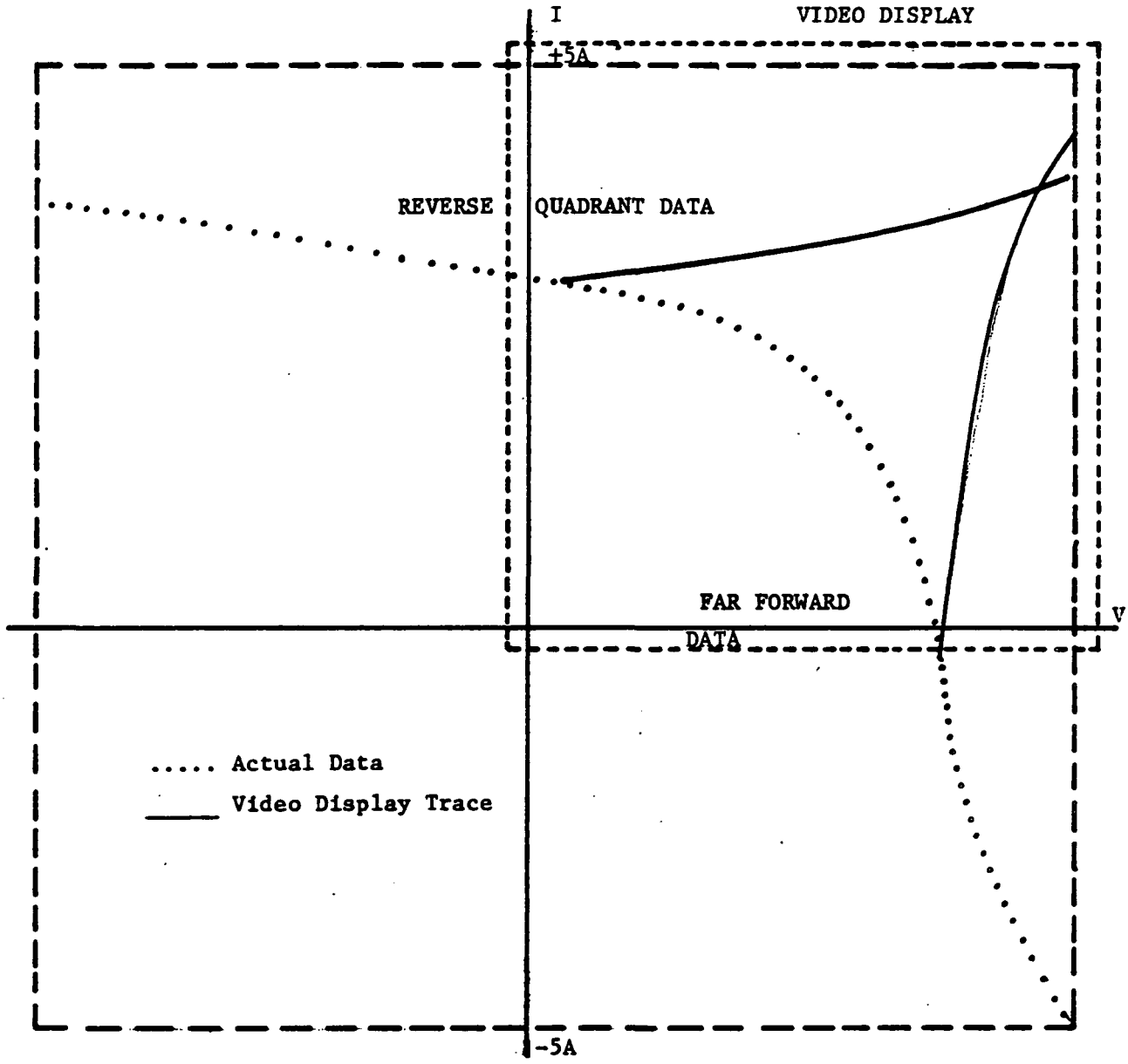

Figure 21. Graphical Representation of 2nd, 3rd and 4th Quadrant Data

degradation mechanisms if it is possible to measure IV characteristics as a function of temperature and noting the differences which result from stressing. Elevated measurement temperatures do not present a problem as it is possible to warm the cells by increasing the temperature of the normal 28 C conditioning air. In a similar fashion the cell may be cooled somewhat below 28 C by chilling the conditioning air. However, when the temperature approaches the ambient dewpoint moisture will condense on the cell surface altering the short circuit current. At a sufficiently low temperature the moisture will form ice crystals, further decreasing the transmission of light. To avoid this problem the cell was mounted on a heat sink which was enclosed, but which had a plexiglass top so the simulator could still illuminate the cell. A photograph of the jig is shown in Figure 22. Methanol, which had been cooled by dry ice, was pumped through the heat sink. The inside of the enclosure was continuously purged with dry (less than 10 ppm H20) nitrogen. When the jig was tested it was found to eliminate moisture condensation on the cell, but at a cell temperature less than -10 C moisture began to condense on the outside of the plexiglass. However, this could be eliminated by blowing slightly warmed air over the outside of the jig enclosure. When making measurements as a function of temperature at elevated temperatures a plexiglass sheet is placed between the light source and cell even though the enclosed jig is not used, to avoid any spectral differences.

Measurement of the characteristics of a:Si cells as a function of temperature is expected to be more difficult because the back surface is not necessarily a good electrical or thermal conductor as is the case in crystalline cells. In addition, the geometry of a:Si cells has not yet been standardized. Variable temperature measurement jigs for a:Si are presently

Figure 22. Photograph of Low Temperature Measurement Jig for Crystalline Cells

being designed.

3.7 New Clemson Reliability Research Facility

The scanning Auger microscope mentioned in the 4th Annual Report has been delivered and installed. Preliminary analyses have been run of selected a:Si cells to develop proper procedures. In order to acquaint the photovoltaic community with its capabilities a workshop is planned sometime after the first of the year, which will include hands-on experience with the instrumentation. A photograph of the installed Auger microprobe is shown in Figure. 23.

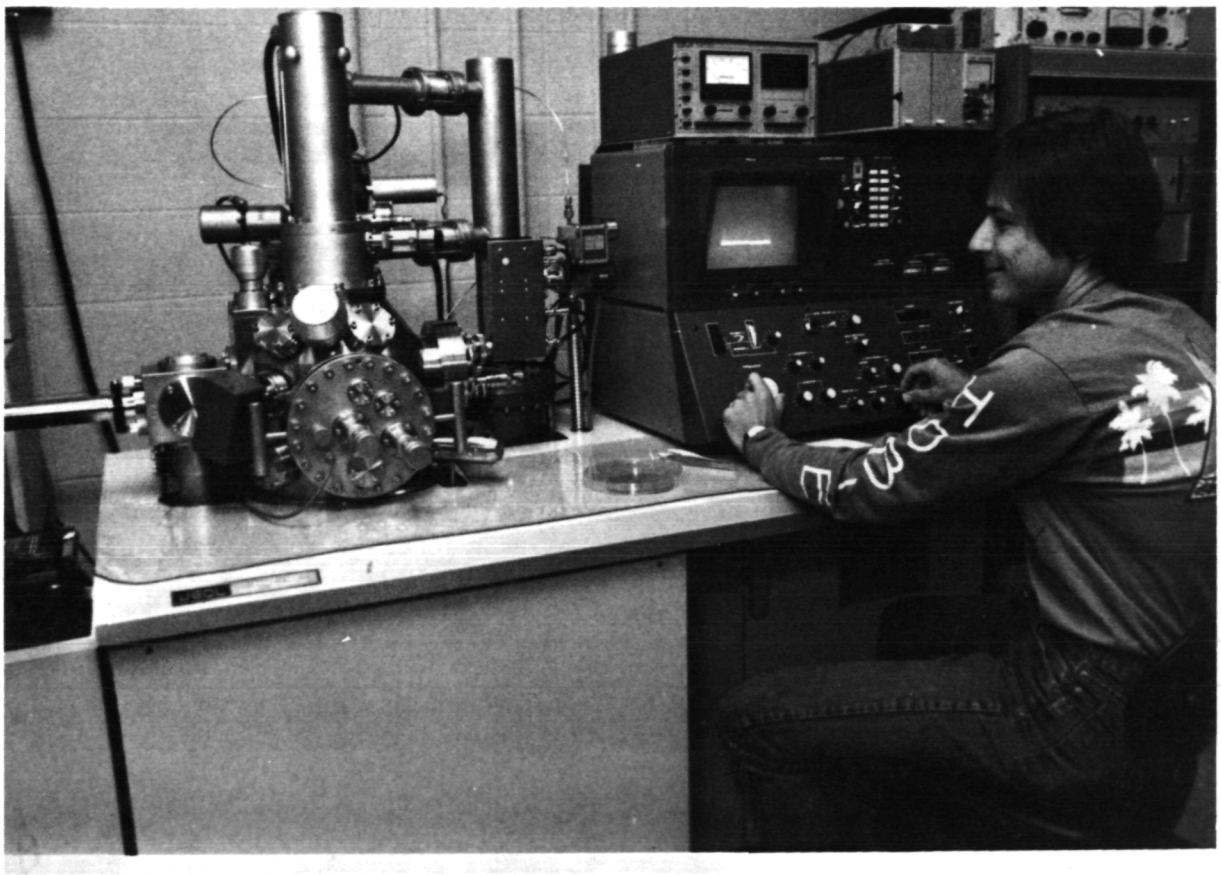

Figure 23. Photograph of Clemson's Auger Microprobe

4.0 CONCLUSIONS

Reliability Research Test Program (Section 2.0) -- Preliminary step stress tests on one submodule have shown the existence of a transition temperature between 130 and 140 C where a sudden change is detected in the electrical characteristics of the cells. This temperature, at which presumably an extraneous degradation mode was introduced, is somewhat lower than the 150 C upper temperature stress used in testing unencapsulated crystalline cells, but at the same time is somewhat higher than the 95 C upper temperature bound for testing encapsulated cells. If this temperature proves to be a real upper bound it will mean that a new accelerated test schedule will need to be developed for a:Si cells.

Reliability Instrumentation Research Program (Section 3.0) -- The two factors which make possible effective accelerated testing are a repeatable measuring system and the existence of a stress window where the stress is sufficiently high to result in a satisfactory acceleration factor, but not so high as to introduce extraneous degradation modes. The major reliability instrumentation research effort during this reporting period was aimed at achieving these two factors relative to thin film a:Si cells. The key to a repeatable measurement system is a stable reference cell with the proper spectral characteristics and an approach to fabricating such a cell from single crystalline silicon is currently being investigated.

Page intentionally left blank

Page intentionally left blank

5.0 NEW TECHNOLOGY

The simulated a:Si reference cell, described in Section 3.2 and illustrated in Figure 7, and its use to obtain uniform illumination with a multiple lamp source, as described in Section 3.3 and illustrated in Figure 13, are considered items of new technology.

Page intentionally left blank

Page intentionally left blank

6.0 PROGRAM RESEARCH CONTRIBUTIONS

Since the previous Annual Report was issued the project has made a number of documented contributions to the photovoltaic community. These are summarized in this section with abstract material reproduced in Appendix B.

Publications and Presentations:

1. Misiakos, K., and Lathrop, J.W., "Barrier Height Determination of Schottky Contacts Formed at the Back Contact-Semiconductor Interface of Degraded Solar Cells," Proceedings of the IEEE Region 3 Conference (SOUTHEASTCON), Louisville, KY, April 1984.

2. Lathrop, J.W., Misiakos, K. and Davis, C.W., "Degradation in Silicon Solar Cells Caused by the Formation of Schottky Barrier Contacts During Accelerated Testing," Proceedings of the 17th Photovoltaic Specialists Conference, Orlando, FL, May 1984.

3. Lathrop, J.W. and Royal, E.L., "Assessment of Degradation in Crystalline Silicon Solar Cells Through the use of an Accelerated Test Program," Proceedings of International PVSEC-1, Kobe, Japan, November, 1984.

4. Lathrop, J.W. and Misiakos, K., "Degradation of Silicon Solar Cells Due to the Formation of Schottky Barrier Contacts," Proceedings of International PVSEC-1, Kobe, Japan, November, 1984.

Theses:

White, F.B., "Design Considerations for a Constant Flow Sulfur Dioxide Accelerated Test System," MS Electrical Engineering Thesis, Clemson University, December 1983.

Misiakos, K., "Schottky Barrier Formation in Terrestrial Solar Cells," MS Electrical Engineering Thesis, Clemson University, August 1984.

Page intentionally left blank

Page intentionally left blank

7.0 REFERENCES

1. Investigation of Reliability Attributes and Accelerated Stress Factors on Terrestrial Solar Cells, DOE/JPL-954929, 1st Annual Report, May 1979.

2. op. cit., 2nd Annual Report, April 1980.

3. op. cit., 3rd Annual Report, January 1981.

4. op. cit., 1981 Summary Report, June 1982.

5. Investigation of Accelerated Stress Factors and Failure/Degradation Mechanisms in Terrestrial Solar Cells, DOE/JPL-954929, 4th Annual Report, October 1983.

APPENDIX A

PUBLICATION ABSTRACTS

1st International Photovoltaic Science and Engineering Conference
Kobe, Japan November, 1984

Degradation of Silicon Solar Cells Due to the Formation of Schottky Barrier Contacts *

Jay W. Lathrop and Konstantinos Misiakos
Electrical and Computer Engineering Department
Clemson University, Clemson, SC 29631 USA

Unencapsulated crystalline silicon solar cells, fabricated by diffusing p-type impurities into a moderately doped n-type substrate, show severe degradation of maximum power output when subjected to accelerated stress testing at elevated temperatures. Examination of degraded cell IV characteristics revealed a peculiar shape in the far forward region. Instead of the continual downward curvature characteristic of normal cells, these degraded cells exhibited an inflection point with an upward curvature at higher voltages. The presence of a reverse curvature of this sort implied that stressing the cells had caused the formation of a Schottky barrier at the ohmic back contact.

Analysis of the IV characteristics of degraded cells at different temperatures permits modelling the Schottky barrier contact and allows calculation of the barrier height. It was found that little or no power loss was observed as long as the saturation current of the Schottky barrier contact was above the short circuit current of the cell, but as the rectifying contact became better, i.e. the saturation current became less than Isc, power loss became apparent. This occurred at an effective barrier height of approximately 0.35 eV. In addition there was evidence of an interfacial layer since the ideality factor was close to 2.

It is hypothesized that the rectifying contact formation mechanism is the saturation of dangling silicon bonds at the interface, causing a reduction in the surface state density. A series of experiments involving different ambients and different encapsulation conditions was performed in an attempt to define the exact mechanism. Although not conclusive, evidence points to the dissociation of water vapor molecules into hydrogen and oxygen at the metal surface with subsequent diffusion of atomic hydrogen through the metal to the semiconductor interface. This would explain the more rapid degradation observed for cells encapsulated with organic or aluminum foil substrates compared to unencapsulated cells. Howerver, oxygen may also play a role in causing degradation.

* This work supported in part by JPL under Contract 954929

1st International Photovoltaic Science and Engineering Conference
Kobe, Japan November, 1984

P.1

Assessment of Degradation in Crystalline Silicon Solar Cells Through the Use of an Accelerated Test Program *

J.W. Lathrop
Electrical and Computer Engineering Department
Clemson University, Clemson, SC 29631 USA

E. Royal
Jet Propulsion Laboratory, MS 506-328
4800 Oak Grove Drive, Pasadena, CA 91109 USA

The reliability characteristics of solar cells intended for low-cost terrestrial applications, either central power generation or distributed residential usage, will be a key factor in the determination of the economic feasibility of such systems. Typical cost models are based on a 30-year module life, which is generally accepted to mean that the power output of an array should not decrease by more than 10% during this period. This degree of system reliability requires the use of very stable cells. Clemson University, under JPL sponsorship, has had a program to assess the relative reliablity attributes of crystalline silicon solar cell technology through laboratory accelerated stressing since 1977. This paper discusses the methodology of accelerated solar cell testing, the specific tests which have been developed, and examples of the method's usefulness as applied to state-of-the-art cells.

The program, which is continuing, has thus far tested both encapsulated and unencapsulated individual cells. Twenty-two types of commercially available cells have been tested in unencapsulated form and nine of these have also been tested in encapsulated form. Seven different encapsulation systems were evaluated which used various combinations of glass, steel, Tedlar ,and aluminum foil with EVA and EMA potting compounds. The significant failure modes observed are discussed and interpreted in terms of physical and chemical effects.

* This work supported in part by JPL under Contract 954929.

17th Photovoltaic Specialists Conference
Orlando, FL May 1984

DEGRADATION IN SILICON SOLAR CELLS CAUSED BY THE FORMATION OF SCHOTTKY BARRIER CONTACTS DURING ACCELERATED TESTING *

J. W. Lathrop, K. Misiakos, and C.W. Davis

Department of Electrical and Computer Engineering
Clemson University, Clemson, SC 29631
(803) 656-3375

EXTENDED ABSTRACT

Using laboratory accelerated testing procedures, Clemson University has been conducting reliability research aimed at understanding failure/ degradation mechanisms which occur at the basic cell level. This paper describes a new degradation mechanism recently found in one type of cell construction. Cells subjected to accelerated stress conditions display severe Pm degradation accompanied by the formation of a distinctly non-linear IV characteristic indicating the formation of a rectifying Schottky barrier at the back contact. The cell had a lightly doped substrate (no back surface field) and relied on a high concentration of surface states, obtained by sandblasting the substrate prior to plating the contact, to give a low barrier height and consequent ohmic contact. This paper describes the degradation effect and offers an explanation for its occurrence.

If the high concentration of surface states is reduced for any reason the barrier height will rise. On lightly doped substrate material it is possible for the barrier to become sufficiently high that Schottky barrier rectification will occur between the back metal contact and the semiconductor substrate. This rectification manifests itself as an unusual non-linearity in the cell's VI characteristic, specifically as an upward concavity to the characteristic in the 4th quadrant (V Voc). Simple computer modelling of a degraded VI characteristics using SPICE, gave an excellent fit provided a poor diode, i.e. one with high leakage, were in series with the back contact.

It has been reported in the literature (1) that surface states result from dangling silicon bonds at the surface. Presumably sandblasting, which damages and distorts the lattice at the surface, increases the number of surface states. It is felt that impurity atoms from the test environment, most likely hydrogen from dissociated water vapor molecules, diffuse through the metal contact to the semiconductor interface, tying up the unshared silicon electrons and reducing the concentration of surface states. This increases the barrier height and results in a rectifying Schottky barrier.

When encapsulated cells were subjected to 85 C/85%RH stress, cells having

an hermetic substrate such as glass or steel showed reduced Pm degradation, whereas those with non-hermetic substrates such as Tedlar showed appreciably greater degradation than even the unencapsulated controls. The reduced degradation observed with hermetic substrates confirms that the effect is moisture related. The increased effect observed with non-hermetic substrates is reasoned to be due to the large difference between diffusion coefficients of water vapor and hydrogen through organic materials. Water vapor is able to easily penetrate the organic encapsulant and reach the metal surface where it dissociates into hydrogen and oxygen molecules which, because of lower diffusion coefficients, become trapped at the interface. A higher concentration of hydrogen at the substrate - contact interface permits a more rapid saturation of the silicon dangling bonds at the metal - semiconductor interface.

Analagous reasoning can also explain the observation that foil substrates did not offer hermetic protection. Cells encapsulated with foil substrates degraded as fast or faster than those with non-hermetic substrates. It is reasoned that the 1-mil thickness of aluminum encased in an organic coating effectively blocks water molecules, but permits penetration of hydrogen atoms.

---

(1) Harrington, W.L. et al, "Low-energy Ion Scattering Spectrometry (Iss) of the SiO2/Si Interface," Applied Physics Letters, vol. 27, p.644 (1975)

* The research described in this paper was supported by the Jet Propulsion Laboratory of the California Institute of Technology and was sponsored by the Department of Energy through an interagency agreement with NASA.

S5-44
ABSONLY
185958
P-1

IEEE Region 3 Conference (SOUTHEASTCON)
Louisville, KY April 1984

Barrier Height Determination of Schottky Contacts Formed at the Back Contact-Semiconductor Interface of Degraded Solar Cells *

K. Misiakos and J.W. Lathrop
Department of Electrical and Computer Engineering
Clemson University, Clemson, SC 29631
(803) 656-3376

ABSTRACT

Solar cells which have degraded as a result of accelerated environmental testing often exhibit a non-linear VI characteristic indicating the formation of a rectifying Schottky barrier at the back contact. In order to study the fundamental physical, chemical, and metallurgical mechanisms causing this barrier it is necessary to be able to quantitatively determine the barrier height. This paper describes a technique used to measure the barrier height of a contact even though that contact is physically inseparable from the cell.

The method is based on interpreting the characteristics of degraded cells in terms of an equivalent circuit. The equivalent circuit is shown in Figure 1, where D1 represents the cell's diffused pn junction and D2 represents the Schottky barrier contact which has formed at the cell's back contact. It has been found experimentally that a resistor, R2, shunting D2 must be included. The experimentally observed VI characteristic can be interpreted in terms of this equivalent circuit. As shown in Figure 2, 5 distinct regions of a degraded cell's characteristic can be identified. In regions 1,2, and 3, D2 is strongly forward biased while in regions 3,4, and 5, D1 is strongly forward biased. In region 1, D1 is forward biased, but not conducting appreciably, while region 2 represents the transition of D1 to strong forward conduction. In region 5, D2 is reverse biased and region 4 represents its transition to strong forward conduction. By generating simplified equivalent circuits for the various regions it is possible to determine values for R1 and R2, and the ideality factors and saturation currents of diodes D1 and D2. The barrier height may be determined from a knowledge of the saturation current of D2 as a function of temperature.

The paper illustrates calculation of the Schottky barrier height using experimentally determined VI curves taken at different temperatures. Experimental results are given showing how the barrier height of solar cell contacts change with the amount of applied environmental stress.

* This work supported in part by JPL under Contract 954929